**Supporting Information for:**

# Development of Thiacrown Ligands for Encapsulation of Mercury-197m/g into Radiopharmaceuticals

Parmissa Randhawa[1,2], Cailum M.K. Stienstra[2], Shaohuang Chen[1,2], Yang Gao[3,4], Georg Schreckenbach[3], Valery Radchenko[2,5] and Caterina F. Ramogida[1,2*]

[1] Department of Chemistry, Simon Fraser University, Canada, [2] Life Sciences Division, TRIUMF, Canada, [3] Department of Chemistry, University of Manitoba, Canada, [4] Institute of Fundamental and Frontier Sciences, University of Electronic Science and Technology of China, China, [5] Department of Chemistry, University of British Columbia, Canada

*Correspondence: cfr@sfu.ca

**Contents**

**NMR Characterization** ..... S2
**Mass Spectrometry** ..... S25
**Density Functional Theory** ..... S26
**Radiolabeling and Stability** ..... S29
**References** ..... S32

## NMR Characterization

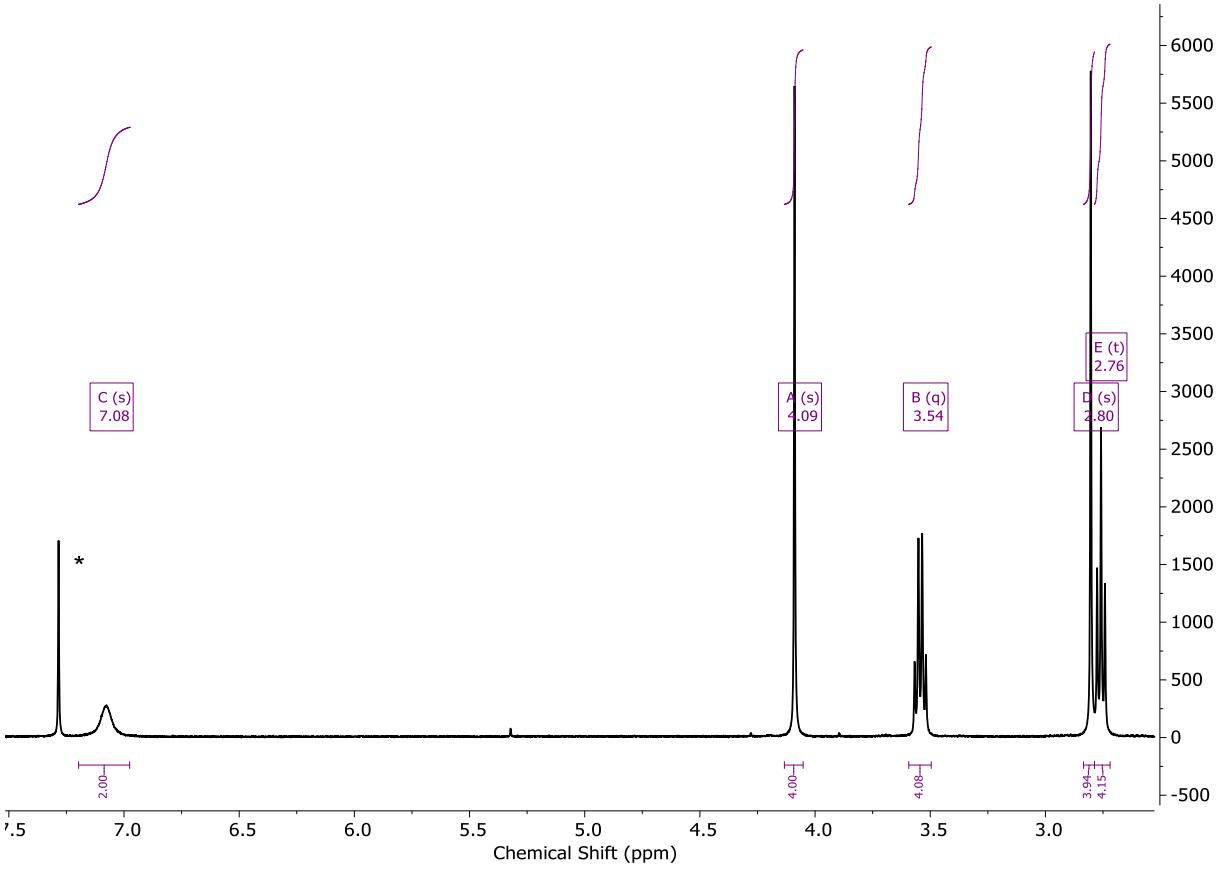


**Figure S1.** $^{1}$H NMR (400 MHz, $CDCl_3$*, 25 ºC): compound **1**.

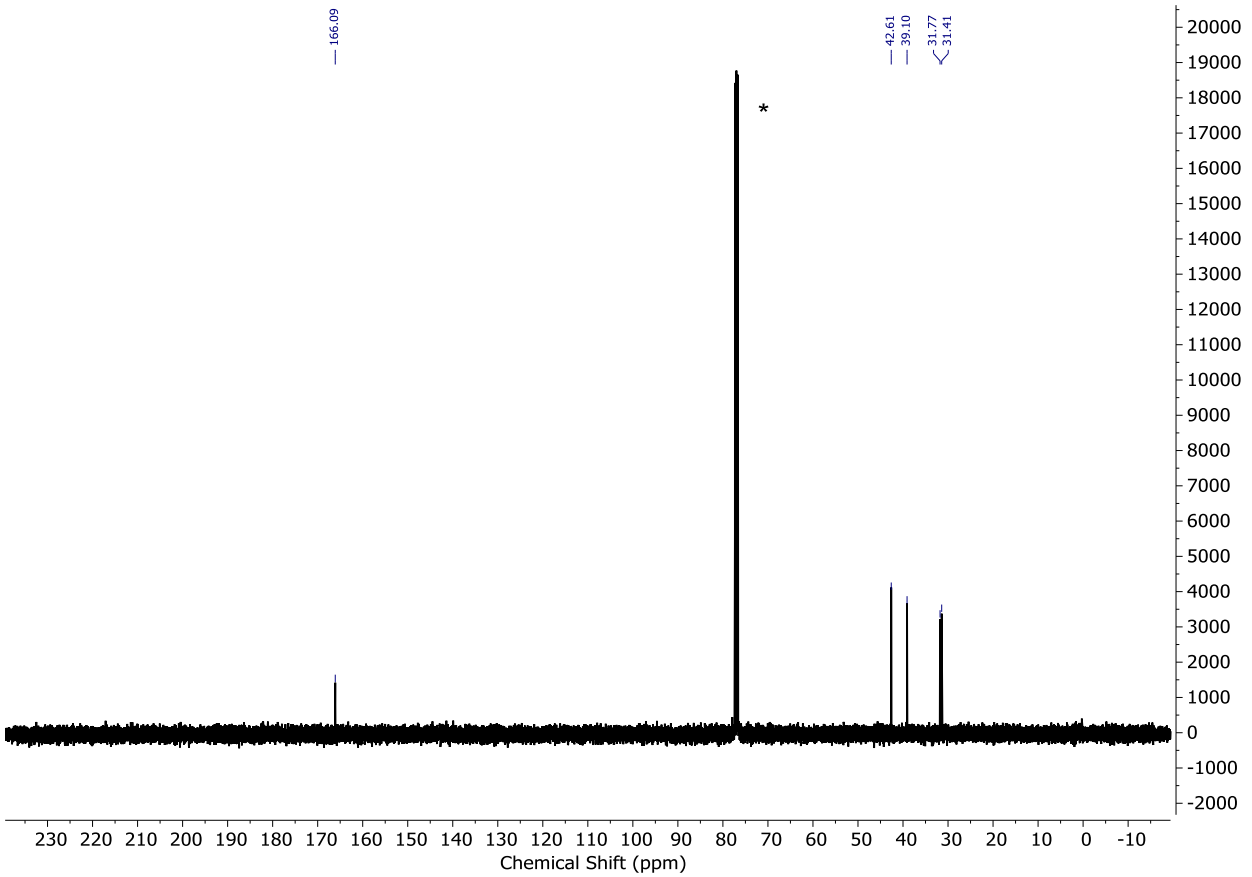


**Figure S2.** $^{1}$H NMR (400 MHz, $CDCl_3$*, 25 ºC): compound **1**.

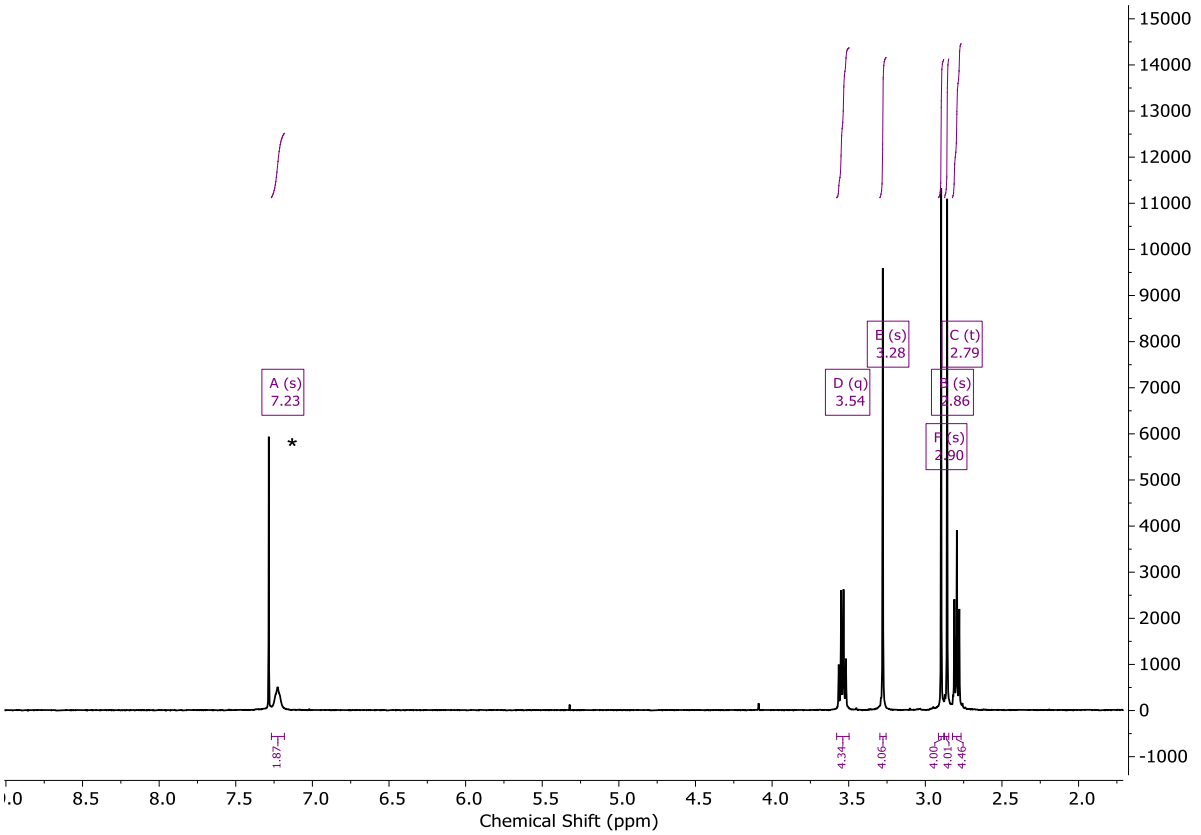


**Figure S3.** $^{1}$H NMR (400 MHz, $CDCl_3$*, 25 ºC): compound **2**.

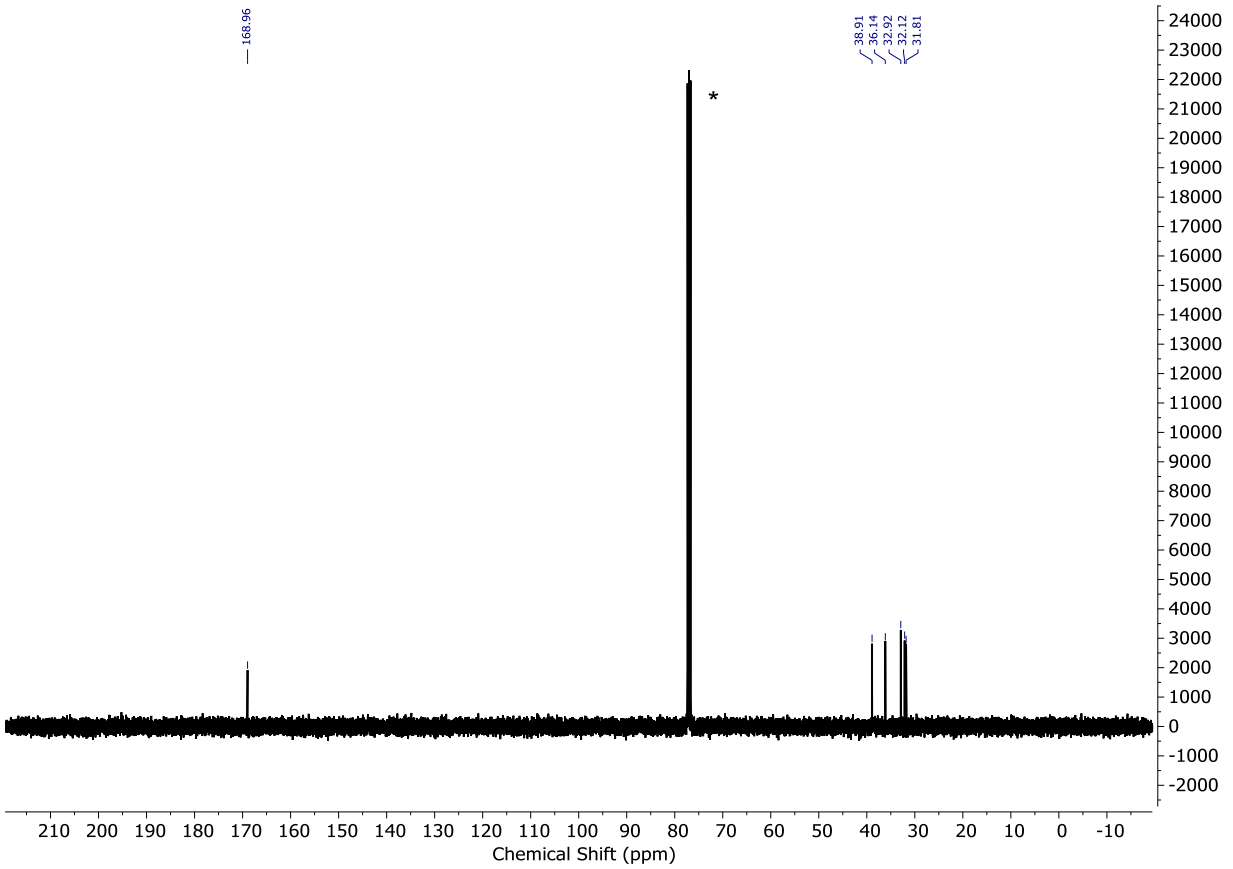


**Figure S4.** $^{13}C\{^{1}H\}$ NMR (101 MHz, $CDCl_3$*, 25 ºC): compound **2**.

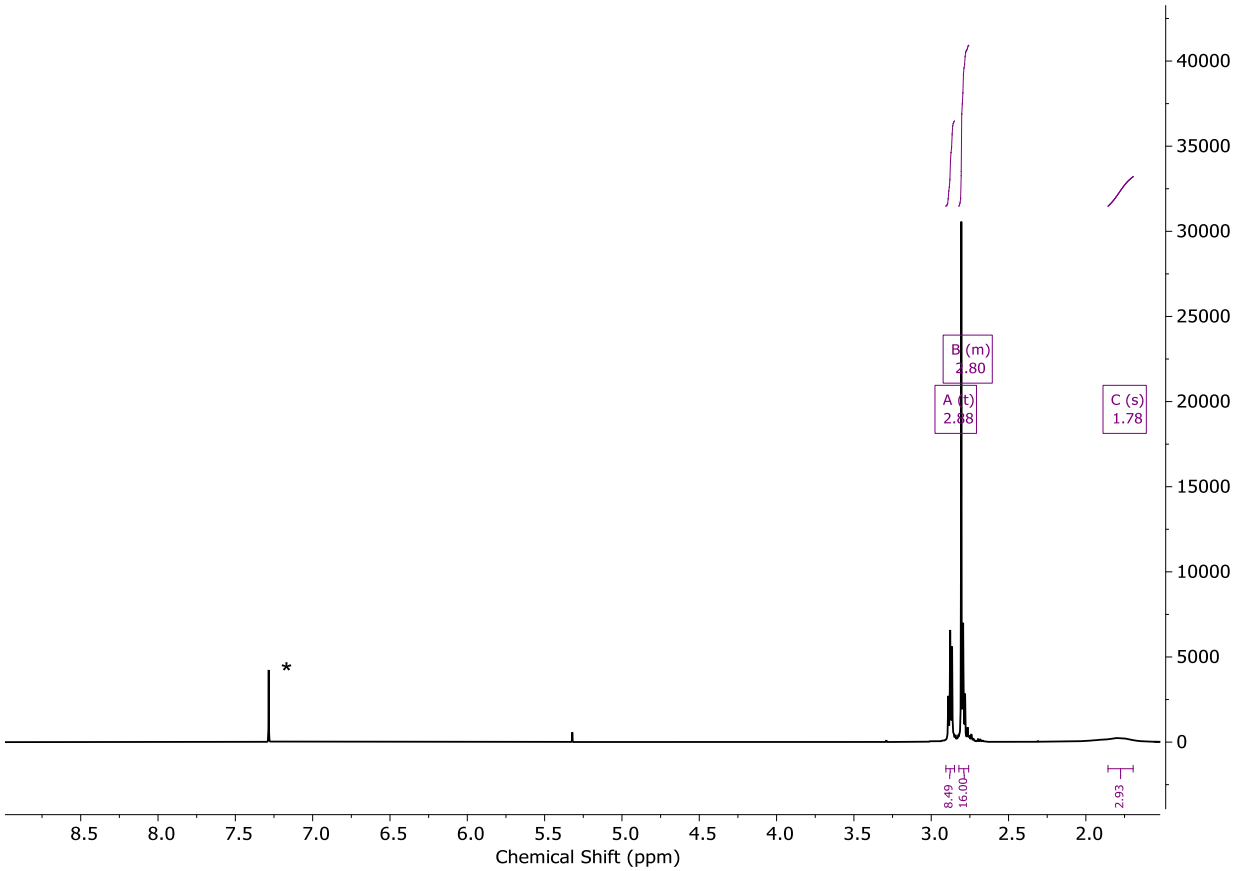


**Figure S5.** $^{1}$H NMR (400 MHz, $CDCl_3^*$, 25 ºC): compound **3**.

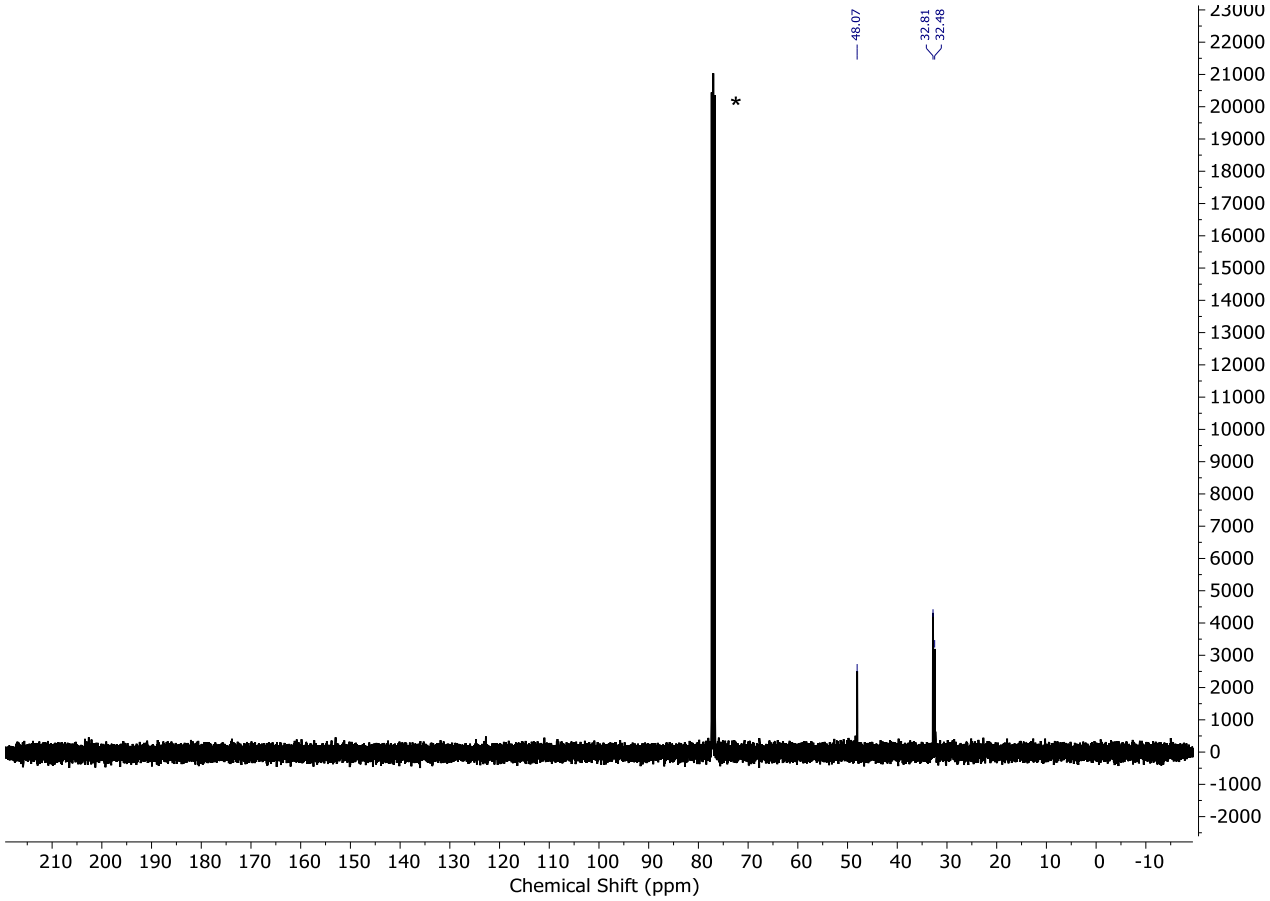


**Figure S6.** $^{13}C\{^{1}H\}$ NMR (101 MHz, $CDCl_3^*$, 25 ºC): compound **3**.

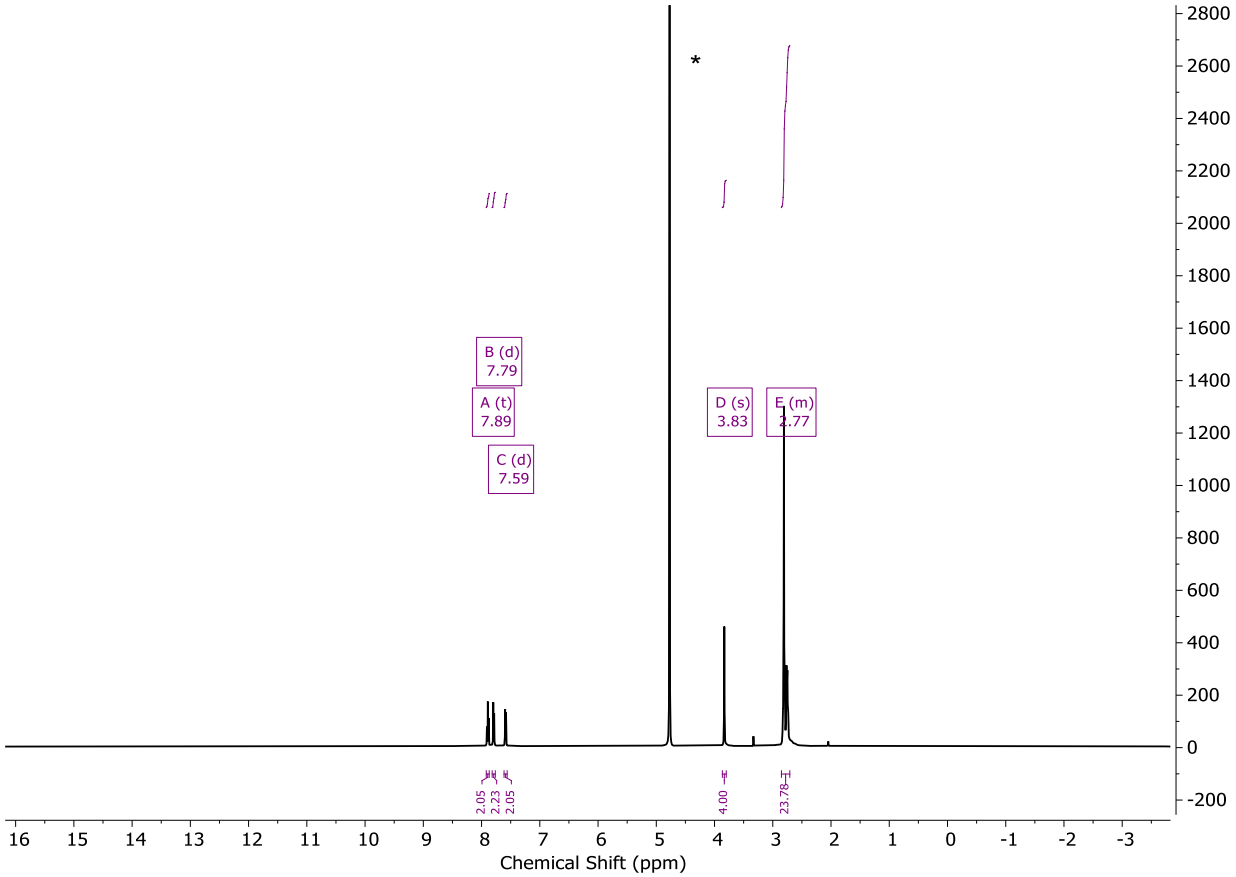


**Figure S7.** $^{1}$H NMR (500 MHz, $D_2O^*$, 25 °C): **$N_2S_4$-$H_2$Pa**.

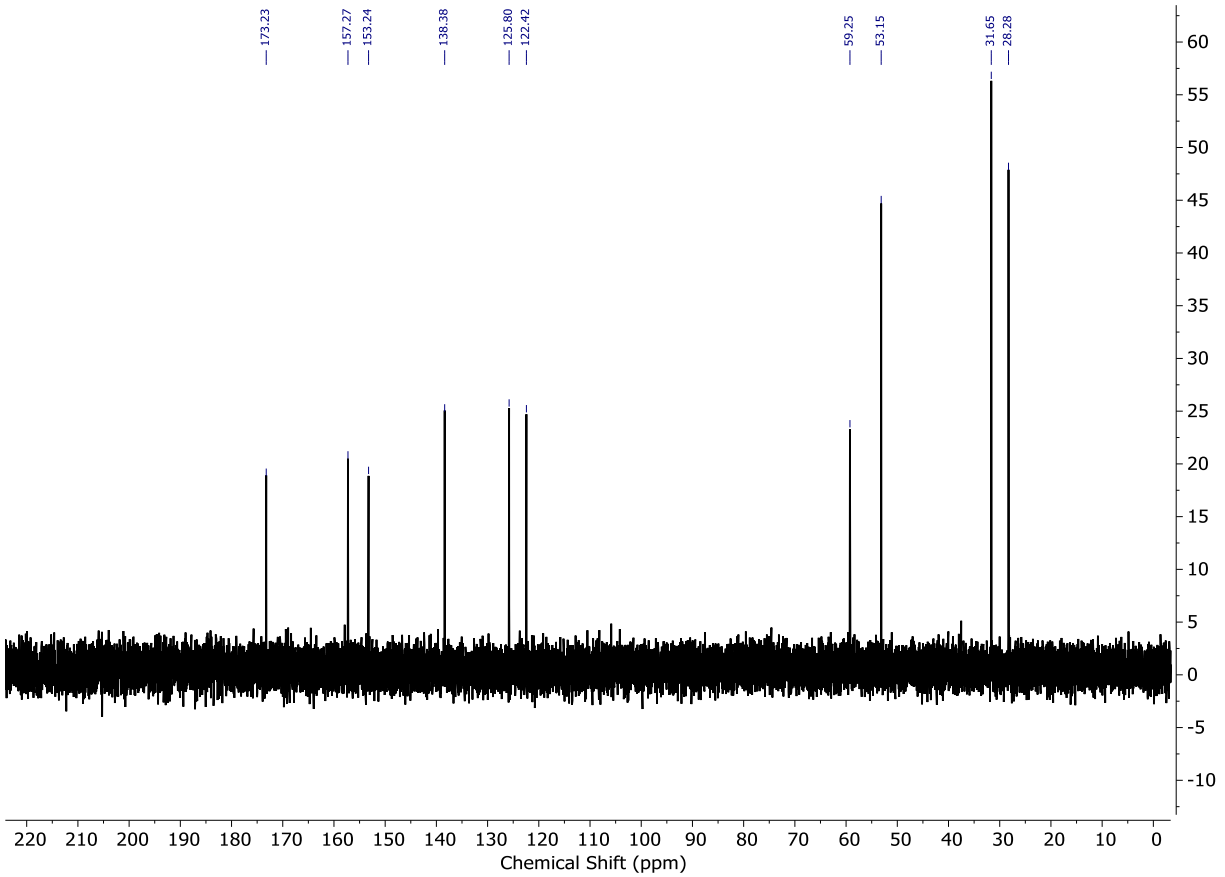


**Figure S8.** $^{13}C\{^{1}H\}$ NMR (126 MHz, $D_2O$, 25 °C): **$N_2S_4$-$H_2$Pa**.

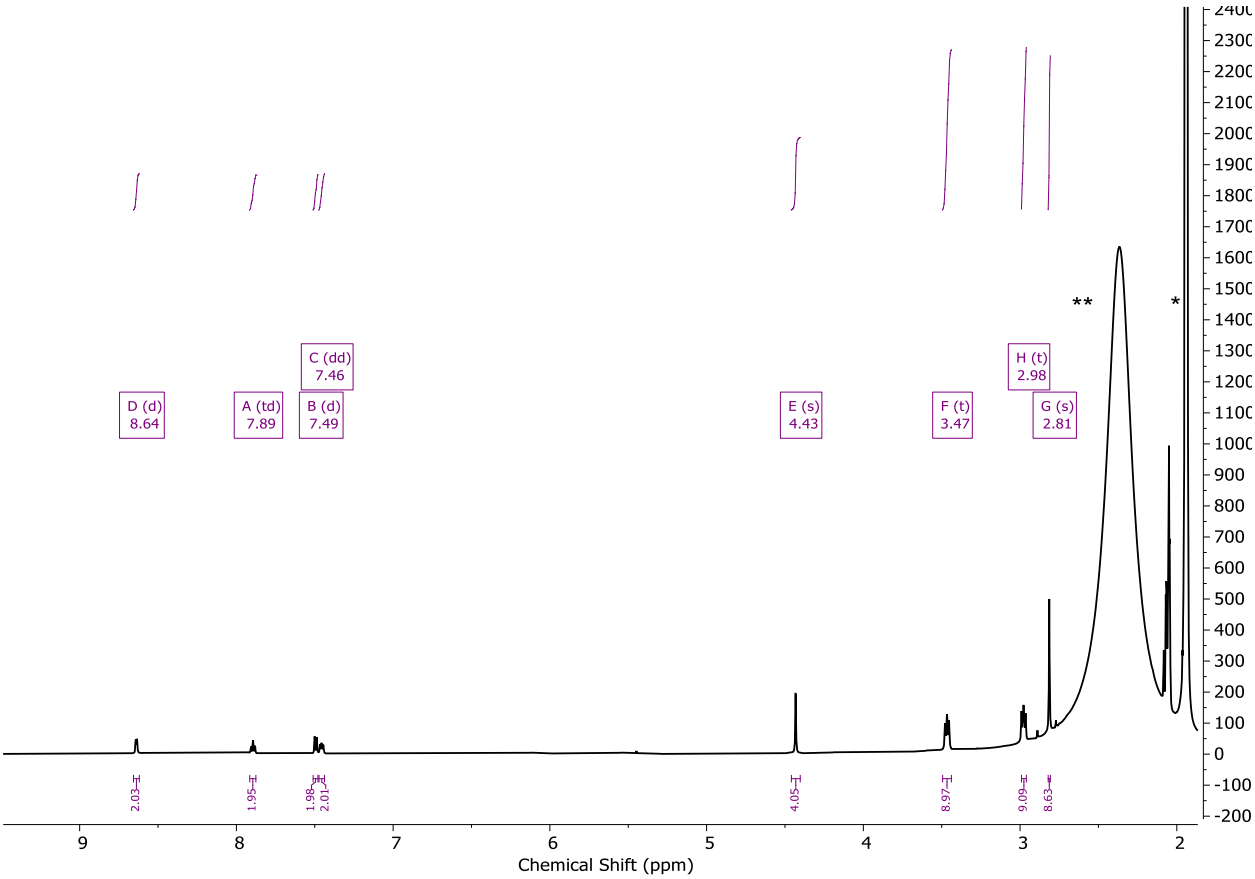


**Figure S9.** $^{1}$H NMR (600 MHz, $CD_3CN^*$, 25 °C): **$N_2S_4$-Py.** (**$H_2O$)

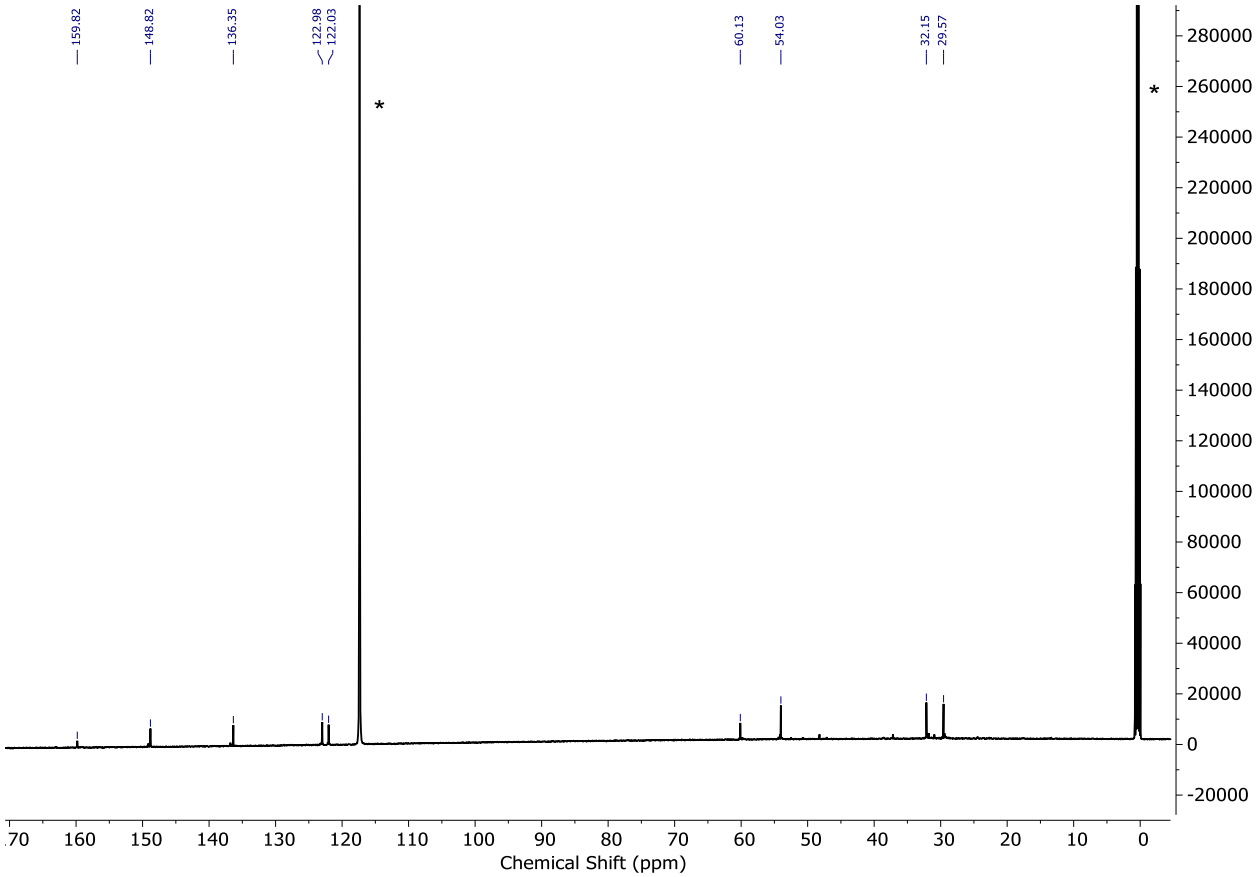


**Figure S10.** $^{13}C\{^{1}H\}$ NMR (151 MHz, $CD_3CN^*$, 25 °C): **$N_2S_4$-Py**.

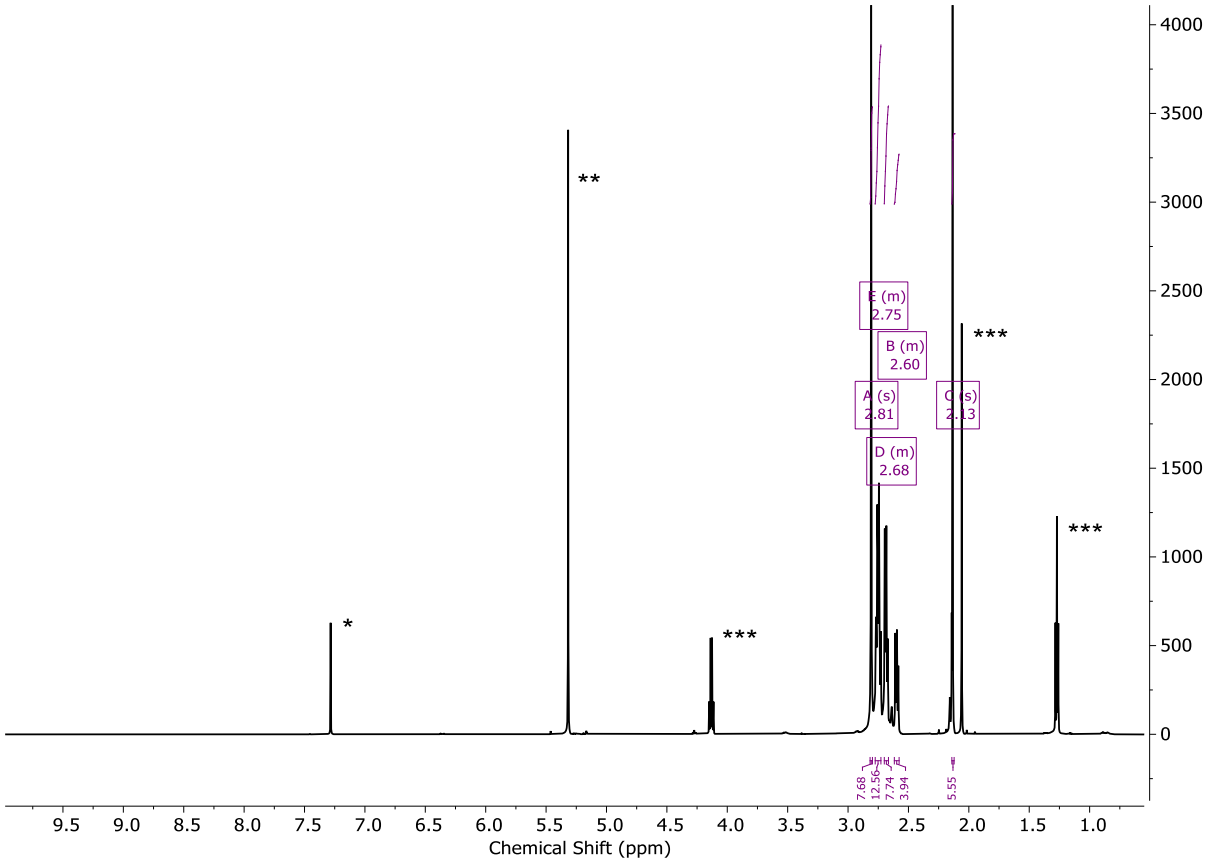


**Figure S11.** $^{1}$H NMR (600 MHz, $CDCl_3$*, 25 ºC): **$N_2S_4$-Thio**. (**$CH_2Cl_2$, ***ethyl acetate)

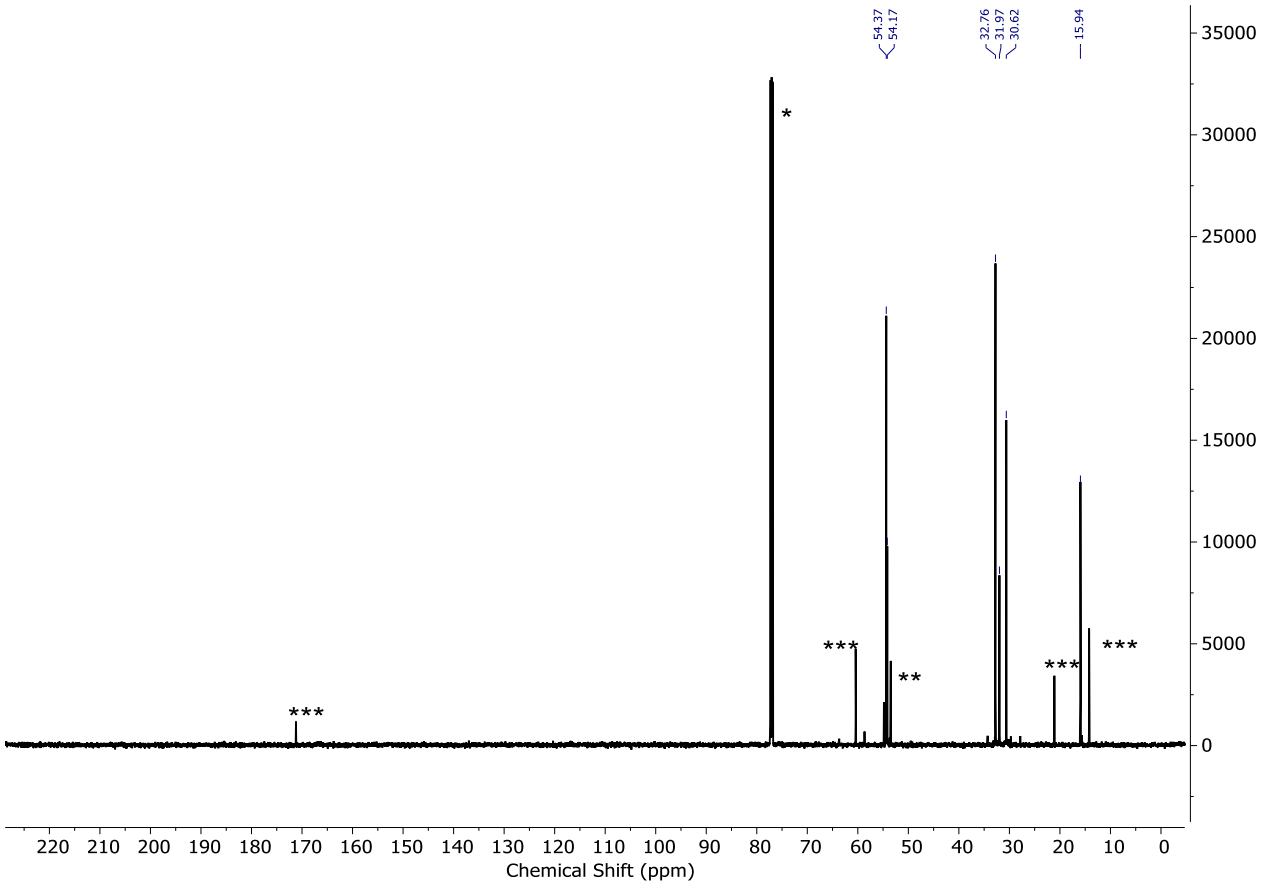


**Figure S12.** $^{13}C\{^{1}H\}$ NMR (151 MHz, $CDCl_3$, 25 °C): **$N_2S_4$-Thio.** (**$CH_2Cl_2$, ***ethyl acetate)

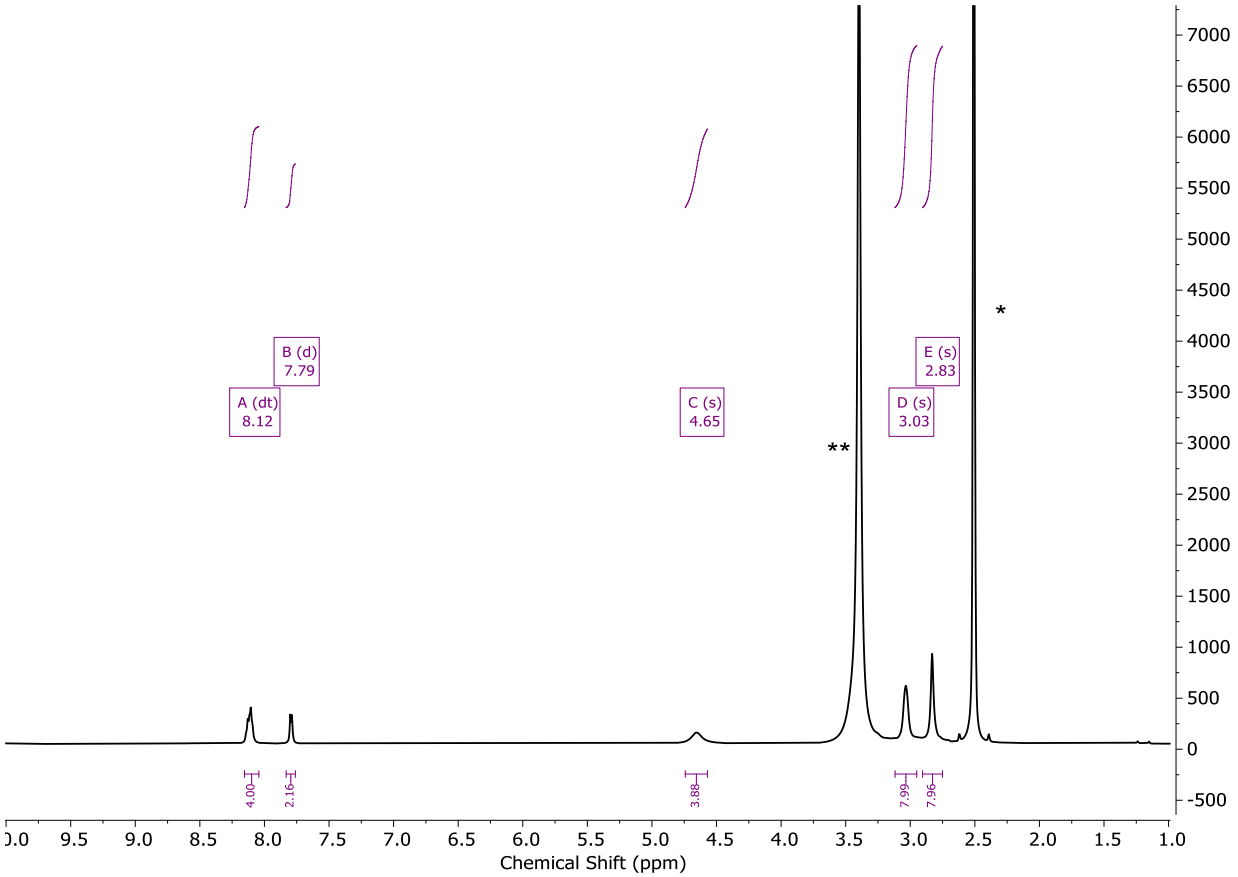


**Figure S13.** $^{1}$H NMR (600 MHz, DMSO-$d_6^*$, 25 °C): **[$^{nat}$Hg($N_2S_4$-Pa)]** at 24 h. (**$H_2O$)

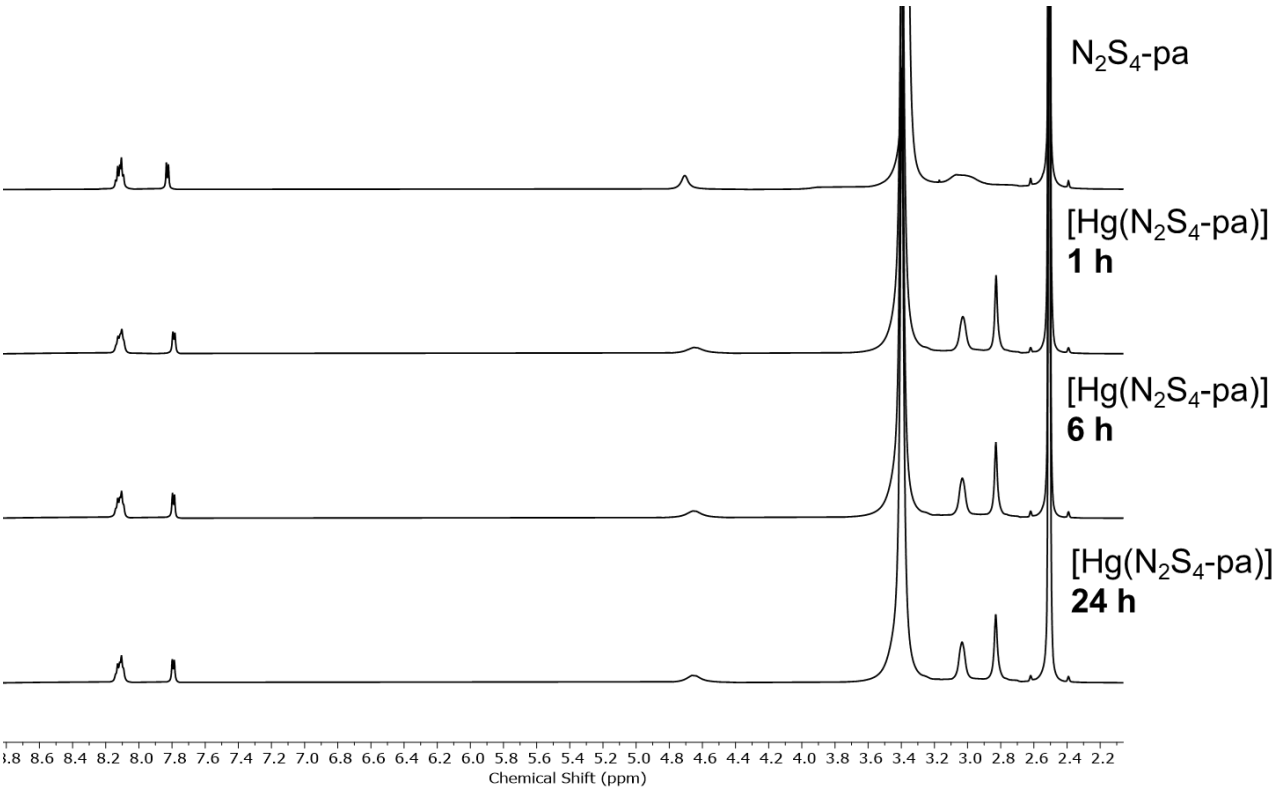


**Figure S14.** $^{1}$H NMR (600 MHz, DMSO-$d_6$, 25 °C): **$N_2S_4$-Pa** and **[$^{nat}$Hg($N_2S_4$-Pa)]** formation over time.

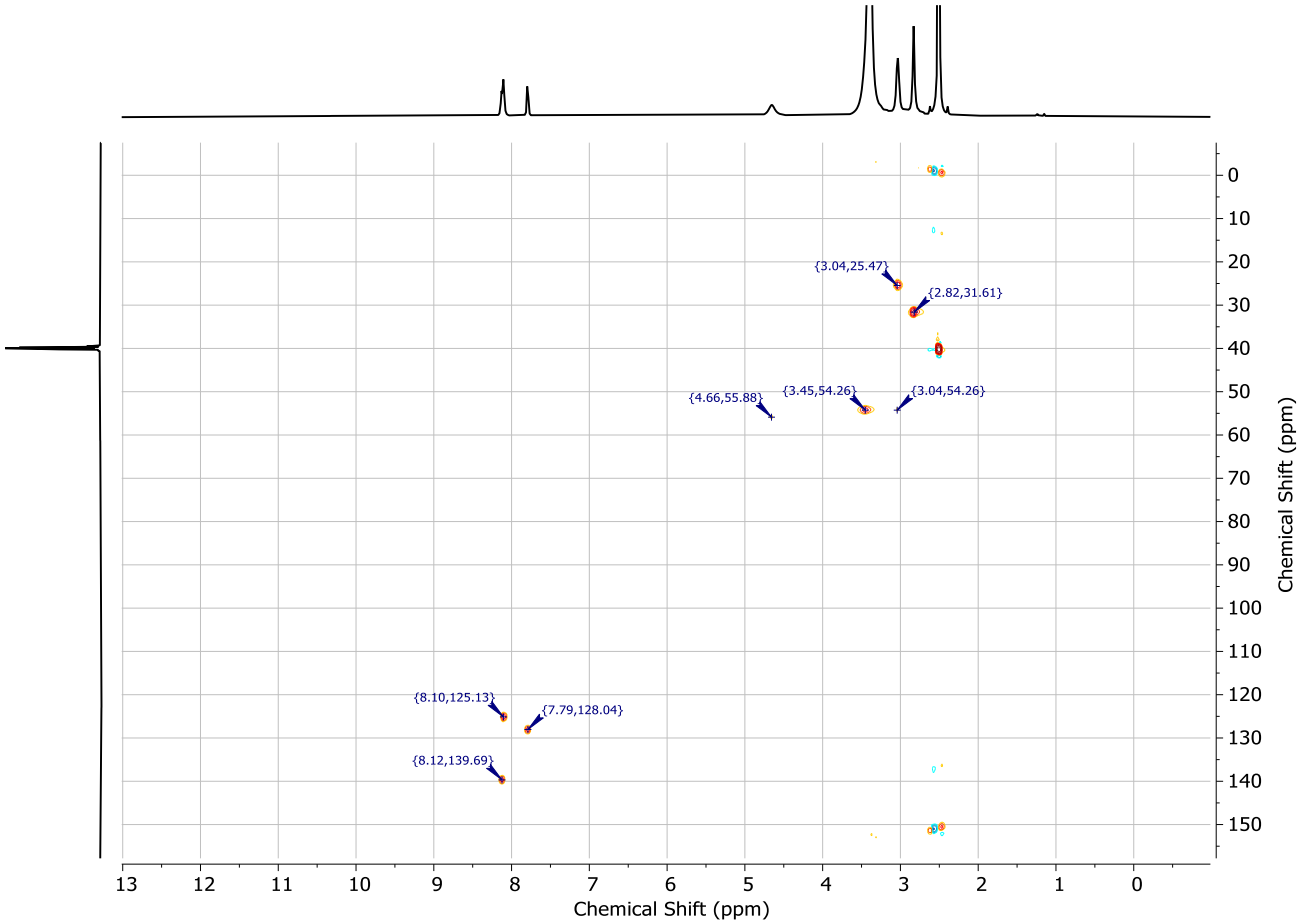


**Figure S15.** $^{1}$H-$^{13}$C HSQC NMR(600 MHz- 161 MHz, DMSO-$d_6$, 25 $^{o}$C): **[$^{nat}$Hg($N_2S_4$-Pa)]**.

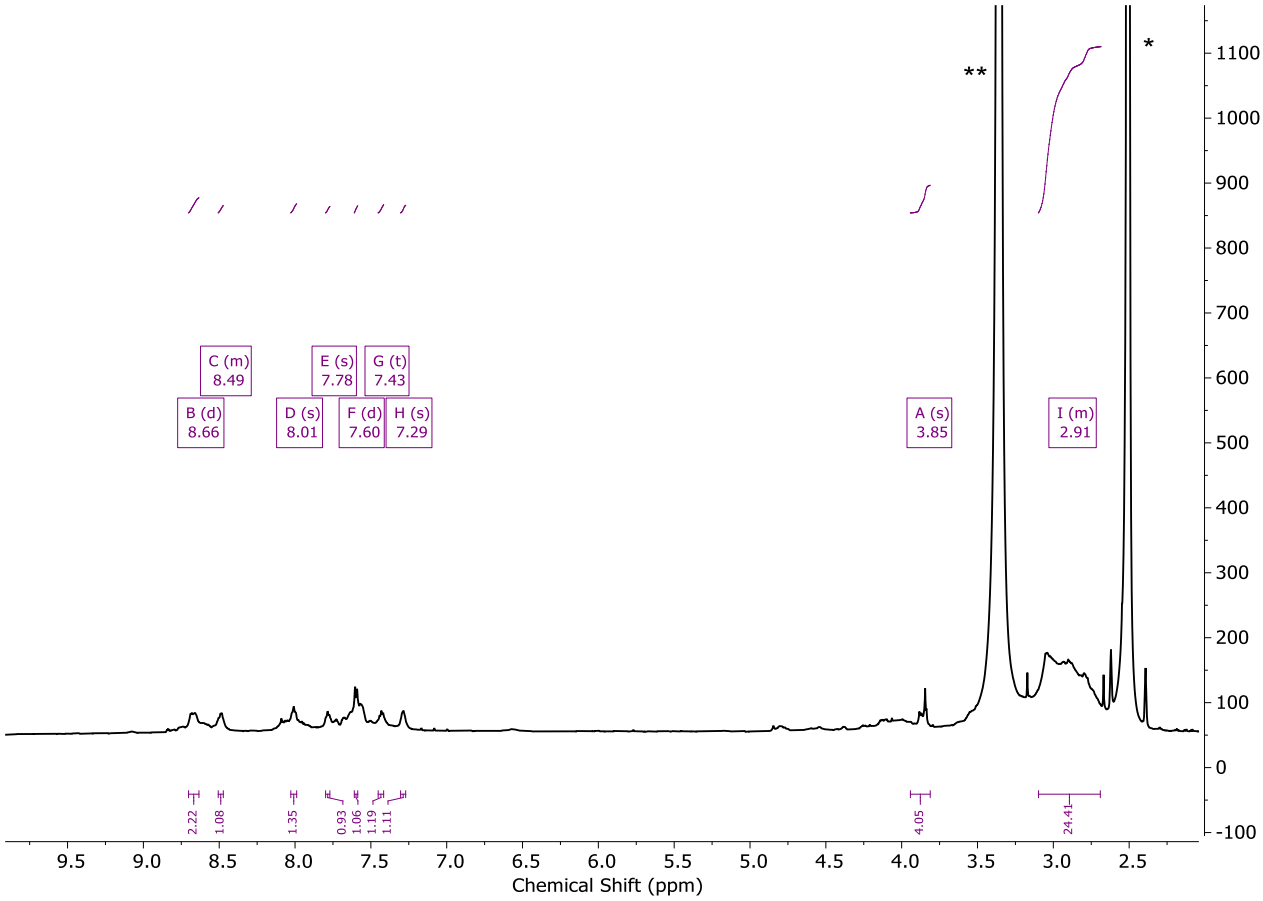


**Figure S16.** $^{1}$H NMR (600 MHz, DMSO-$d_6^*$, 25 $^{o}$C): **[$^{nat}$Hg(N$_2$S$_4$-Py)]$^{2+}$** at 24 h.(**$H_2O$)

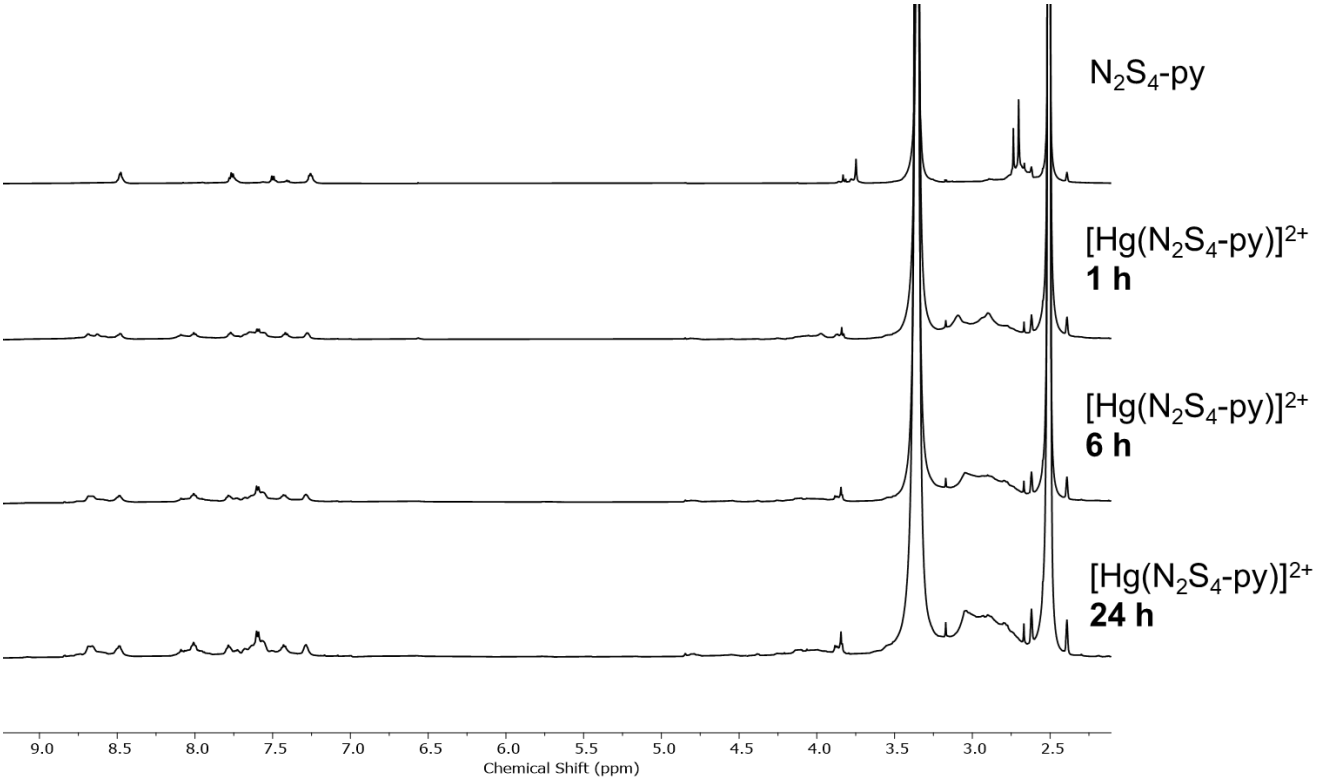


**Figure S17.** $^{1}$H NMR (600 MHz, DMSO-*d*$_6$, 25 °C): **N$_2$S$_4$-Py** and **[$^{nat}$Hg(N$_2$S$_4$-Py)]$^{2+}$** formation over time.

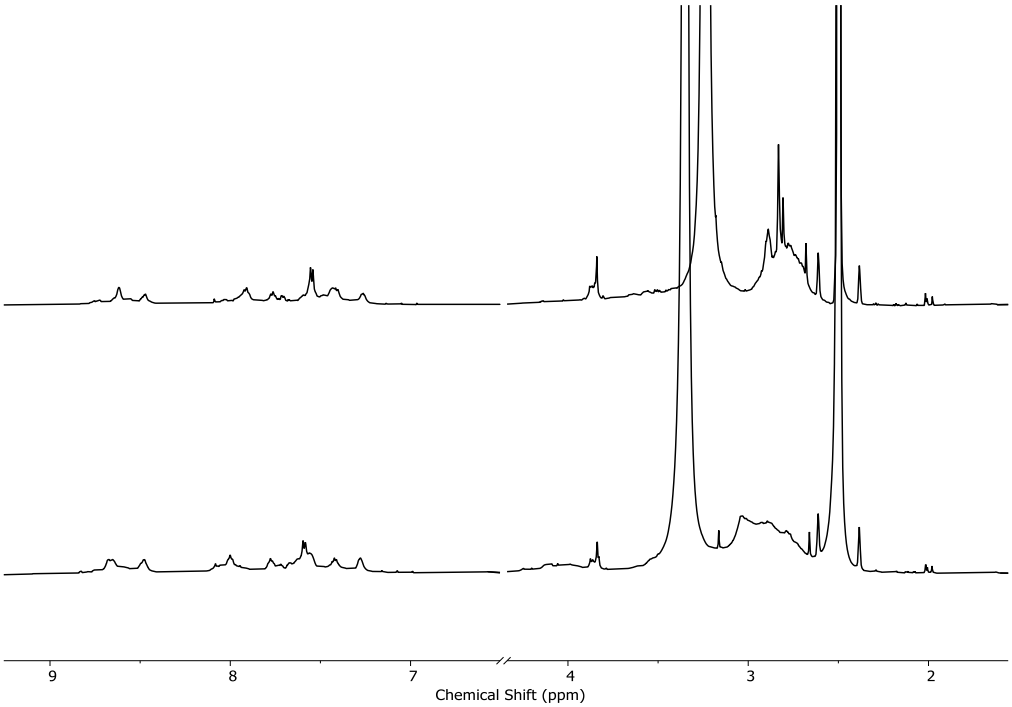


**Figure S18.** $^{1}$H NMR (600 MHz, DMSO-$d_6$): **[$^{nat}$Hg($N_2S_4$-Py)]$^{2+}$** at 45 °C (top) and 25 °C (bottom).

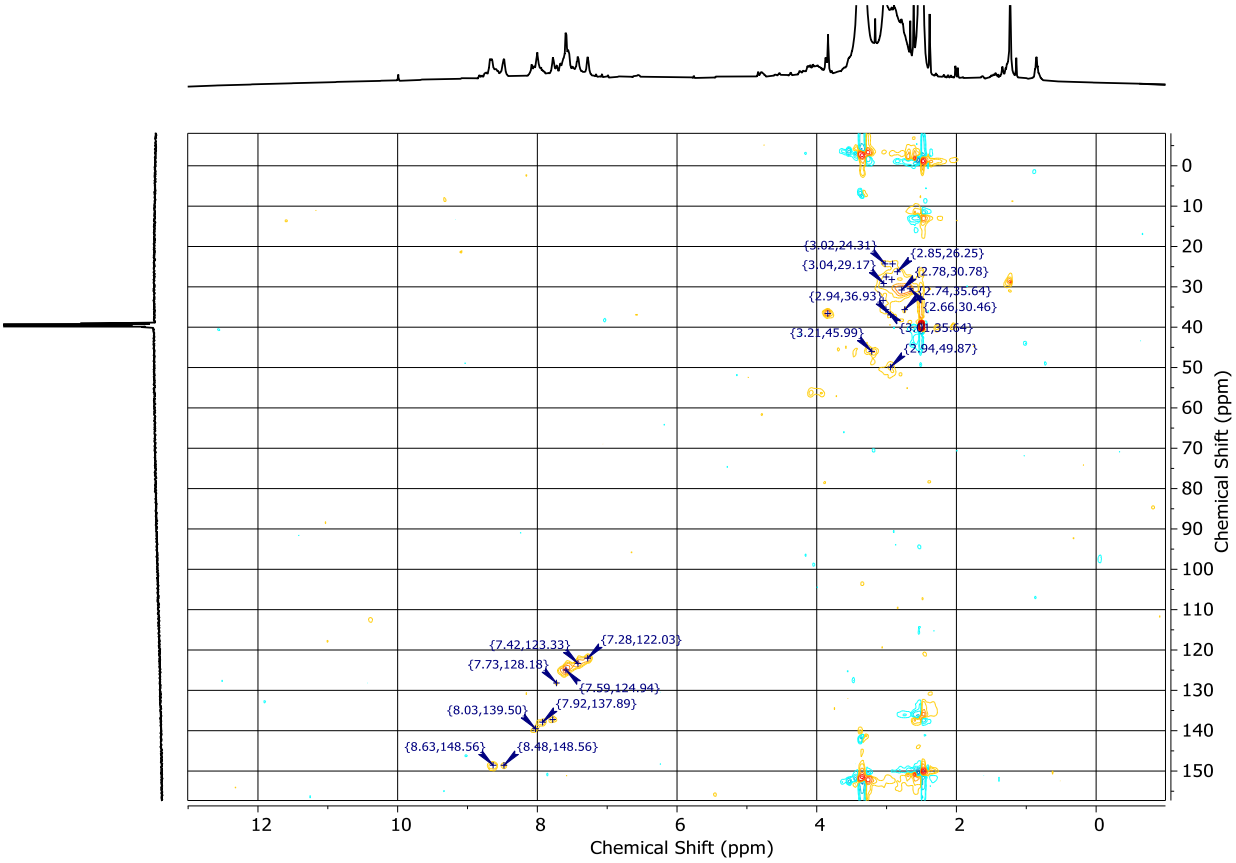


**Figure S19.** $^{1}$H-$^{13}$C HSQC NMR(600 MHz- 161 MHz, DMSO-$d_6$, 25 $^{o}$C): **[$^{nat}$Hg($N_2S_4$-Py)]$^{2+}$**.

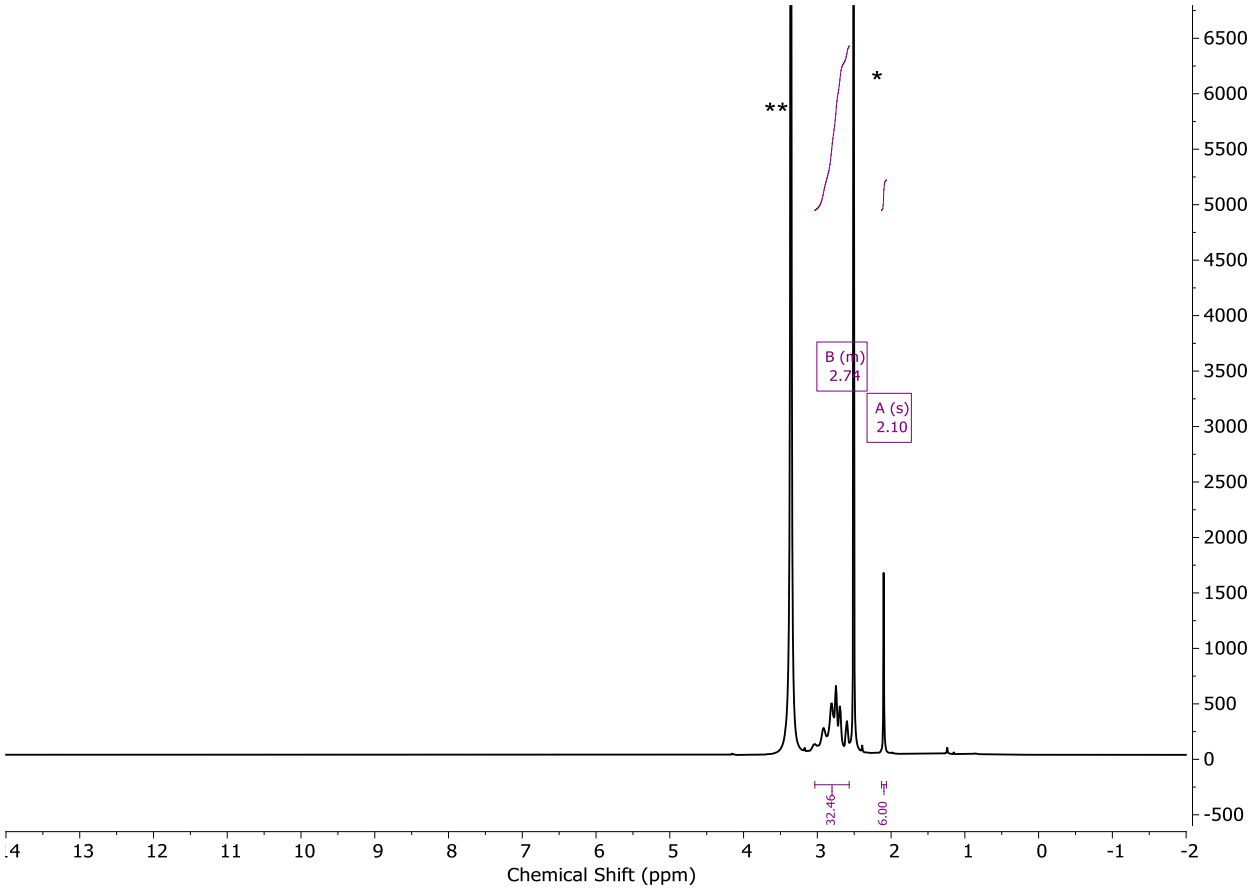


**Figure S20.** $^{1}$H NMR (600 MHz, DMSO-$d_6^*$, 25 °C): **[$^{nat}$Hg(N$_2$S$_4$-Thio)]$^{2+}$** at 24 h.(**$H_2O$)

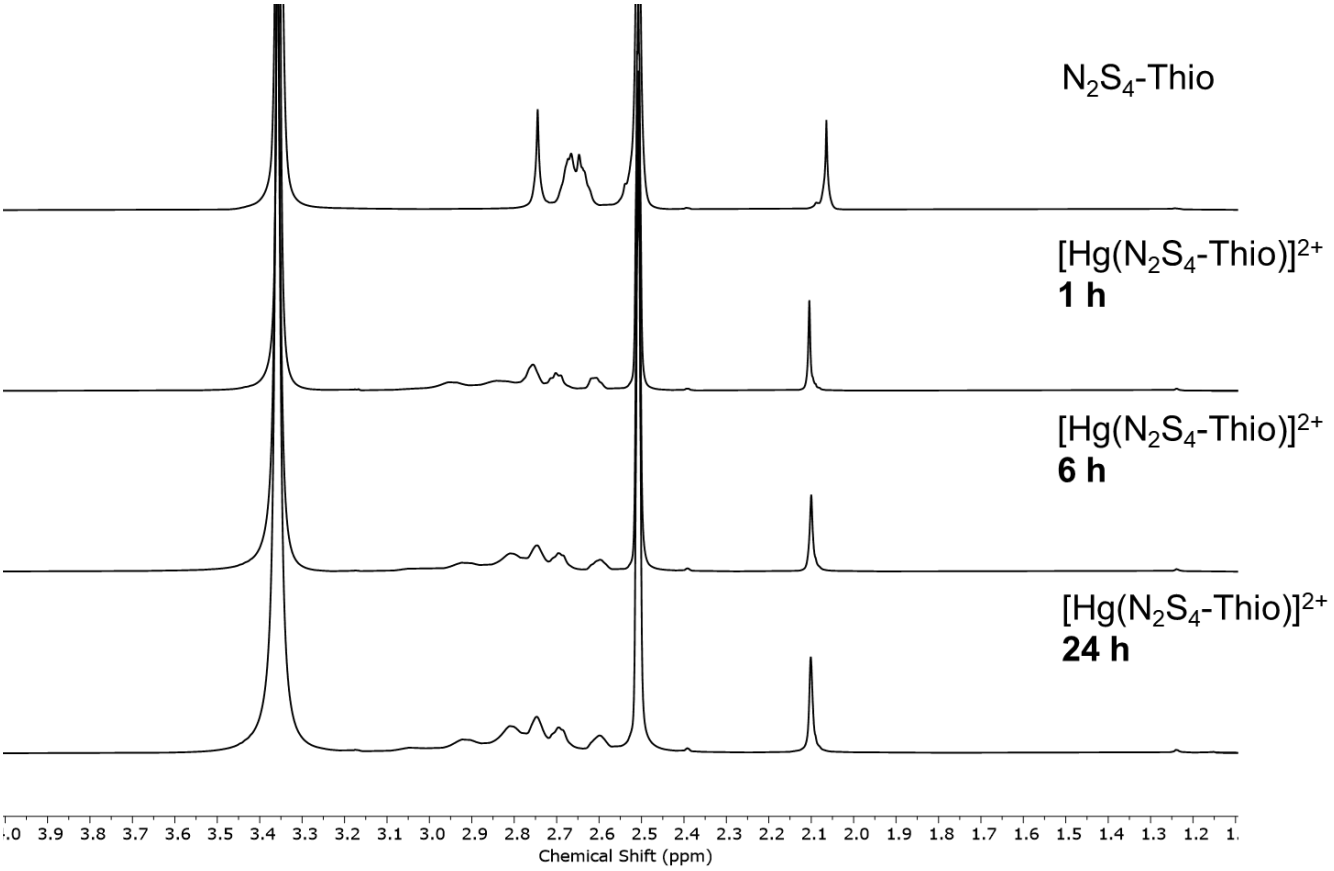


**Figure S21.** $^{1}$H NMR (600 MHz, DMSO-*d*$_6$, 25 °C): **N$_2$S$_4$-Thio** and **[$^{nat}$Hg(N$_2$S$_4$-Thio)]$^{2+}$** formation over time.

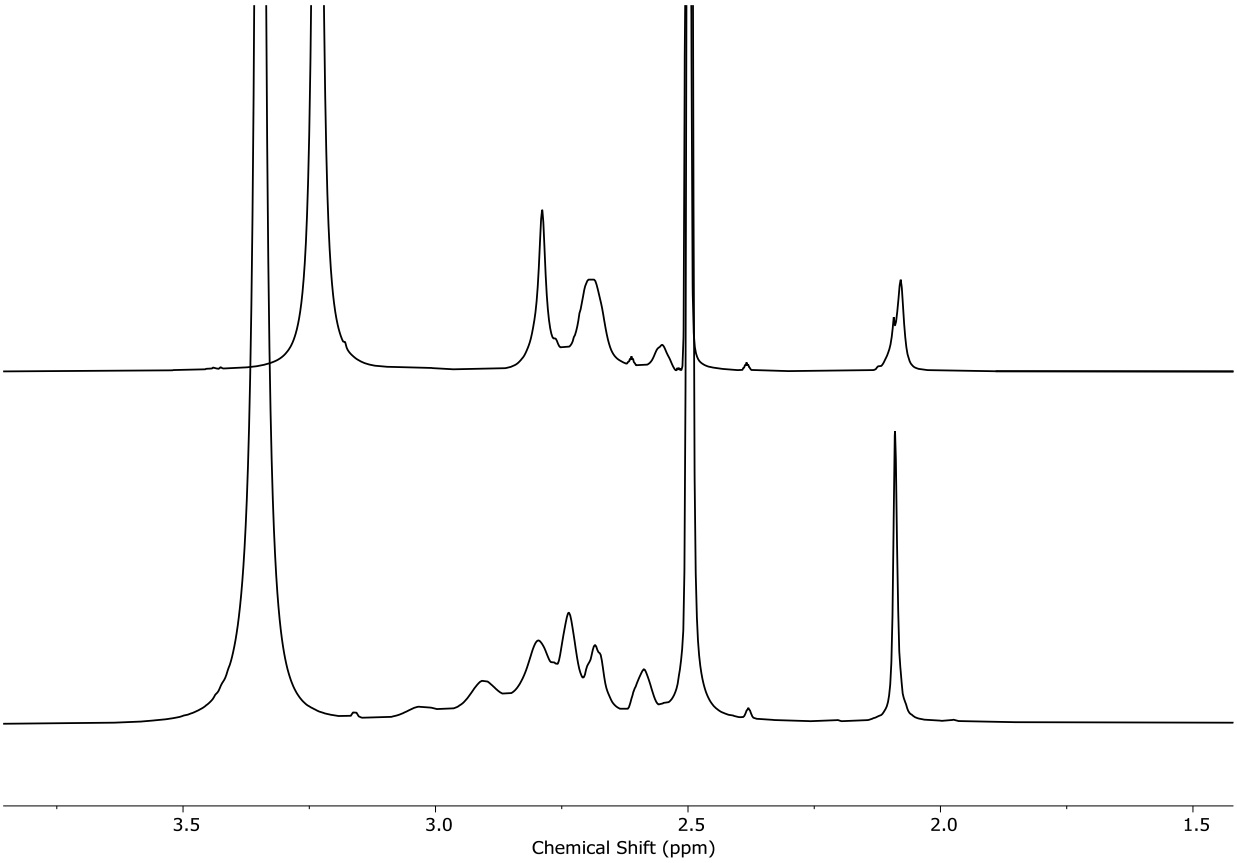


**Figure S22.** $^{1}$H NMR (600 MHz, DMSO-$d_6$): **[$^{nat}$Hg($N_2S_4$-Thio)]$^{2+}$** at 45 °C (top) and 25 °C (bottom).

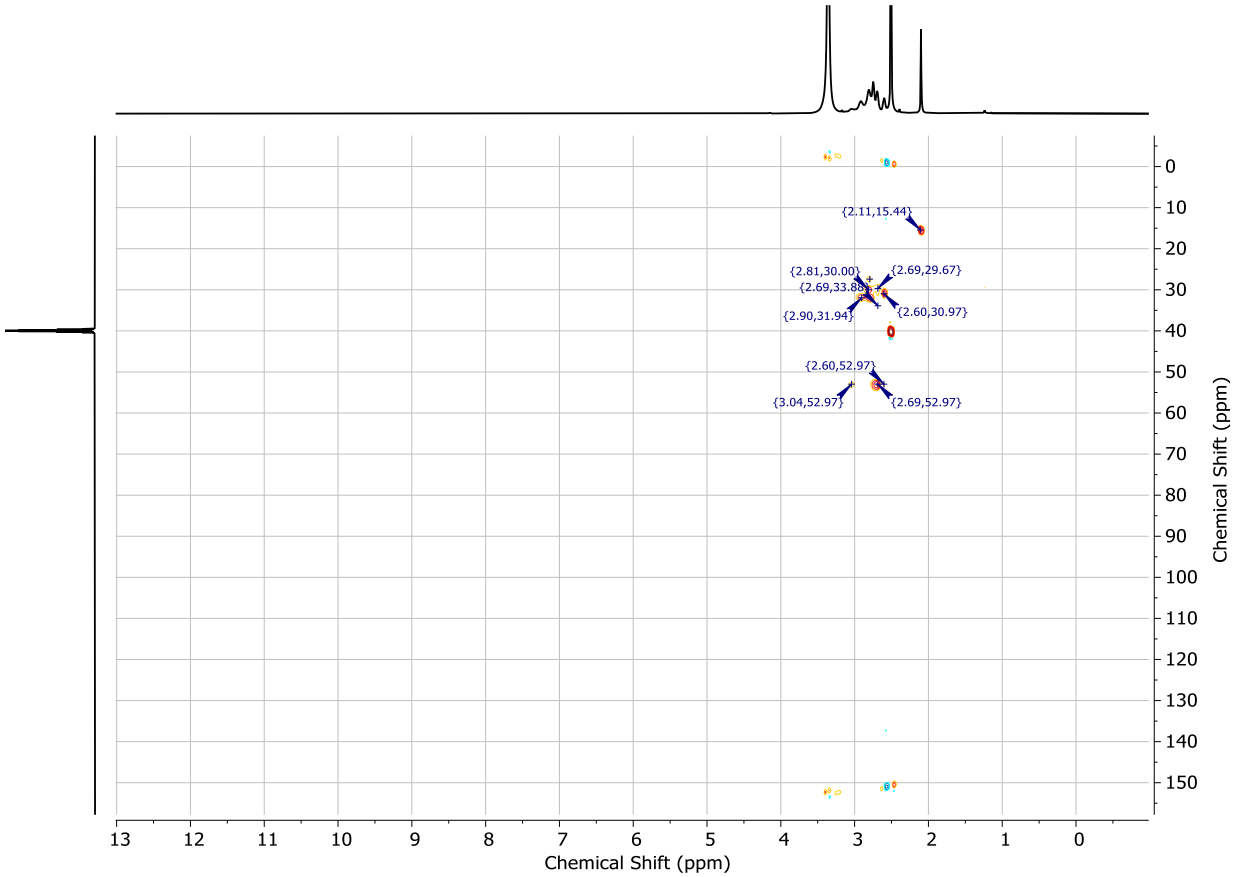


**Figure S23.** $^{1}$H-$^{13}$C HSQC NMR(600 MHz- 161 MHz, DMSO-*d*$_6$, 25 $^{o}$C): **[$^{nat}$Hg(N$_2$S$_4$-Thio)]$^{2+}$**.

## Mass Spectrometry

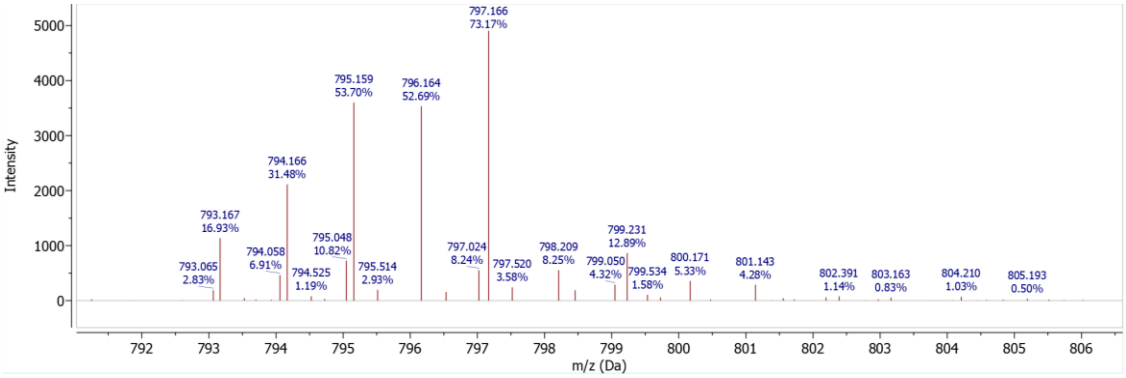


**Figure S24.** HRMS for **[$^{nat}$Hg($N_2S_4$-Pa)]**, ESI-HRMS *m*/*z* calcd. for $[C_{26}H_{34}N_4O_4S_4Hg + H]^+$ 797.125; found 797.166 $[M+H]^+$.

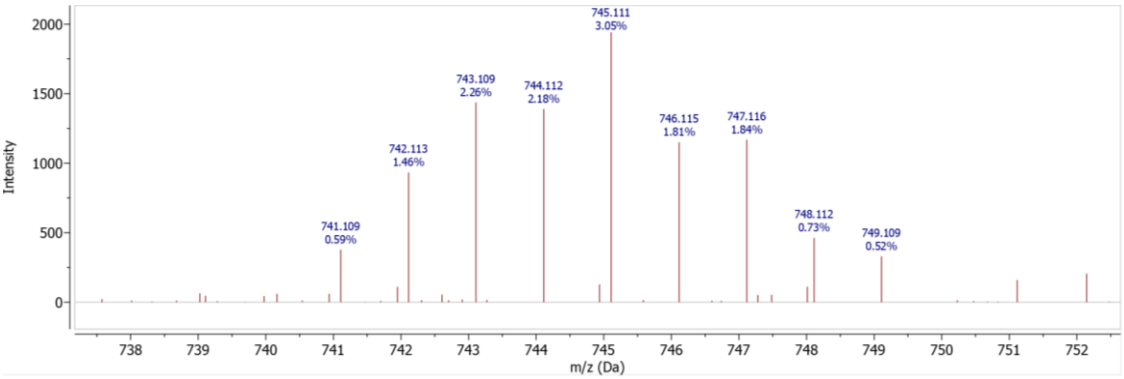


**Figure S25.** HRMS for **[$^{nat}$Hg($N_2S_4$-Py)]$^{2+}$**, ESI-HRMS *m*/*z* calcd. for $[(C_{24}H_{36}N_4S_4Hg)^{2+} + Cl^-]^+$ 745.121; found 745.111 $[M+Cl]^+$.

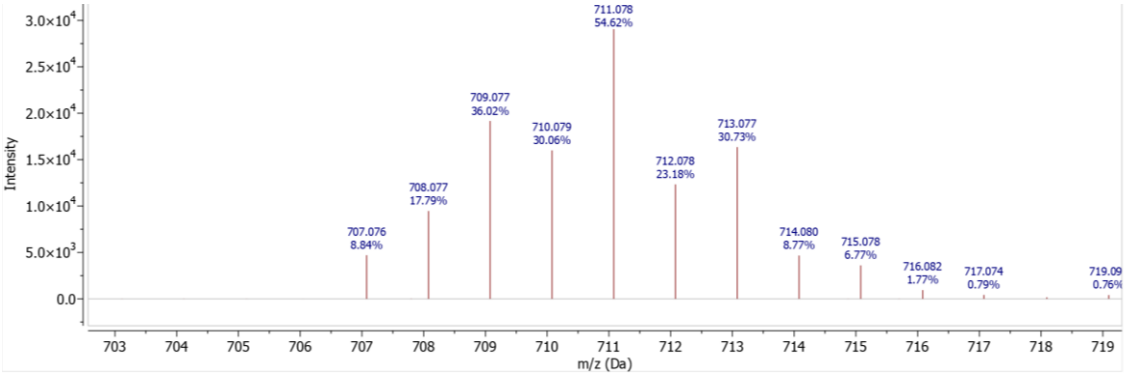


**Figure S26.** HRMS for **[$^{nat}$Hg($N_2S_4$-Thio)]$^{2+}$** ESI-HRMS *m*/*z* calcd. for $[(C_{18}H_{38}N_2S_6Hg)^{2+} + Cl^-]^+$ 711.075; found 711.078 $[M+Cl]^+$.

## Density Functional Theory

$\epsilon_0$ =Electronic energy

$\epsilon_{ZPE}$ =Zero point energy correction

$G_{corr}$= Thermal free energy correction

$\Delta G_{solv}$= Change in energy as a result of solvation

$$G_{gas} = \epsilon_0 + \epsilon_{ZPE} + G_{corr}$$
$$G_{soln} = G_{gas} + \Delta G_{solv} \quad (1)0\ h$$

**Table S1.** Calculated $\Delta G_{gas}$, $\Delta G_{solv}$, $G_{soln}$ and $\Delta G_{soln}$ energies for all investigated conformers of the **[Hg($N_2S_4$-Py)]$^{2+}$** complex. The lowest energy conformation is highlighted in bold.

| Conformer | Sidearm Orientation | Backbone | Relative $G_{gas}$ (kJ/mol) | $\Delta G_{solv}$ (Hartree) | $G_{soln}$ (Hartree) | Relative $G_{soln}$ (kJ/mol) |
|---|---|---|---|---|---|---|
| 1 | cis | λ,λ,δ,λ,λ,δ | 81.3 | -0.22147 | -2901.33939 | 21.1 |
| 2 | trans | δ,λ,λ,δ,λ,δ | 14.3 | -0.19454 | -2901.33798 | 24.8 |
| 3 | cis | δ,λ,δ,λ,λ,δ | 39.4 | -0.20408 | -2901.33799 | 24.8 |
| 4 | trans | λ,λ,δ,δ,λ,δ | 2.2 | -0.19704 | -2901.34511 | 6.1 |
| 5 | cis | δ,λ,δ,λ,λ,λ | 0.0 | -0.19632 | -2901.34522 | 5.8 |
| 6 | trans | λ,λ,λ,δ,λ,δ | 2.3 | -0.19762 | -2901.34564 | 4.7 |
| 7 | cis | δ,λ,δ,δ,δ,δ | 43.6 | -0.20984 | -2901.34213 | 13.9 |
| 8 | trans | δ,λ,λ,δ,δ,δ | 42.2 | -0.20428 | -2901.33711 | 27.1 |
| **9** | **cis** | **δ,λ,δ,λ,δ,δ** | **20.9** | **-0.20647** | **-2901.34743** | **0.0** |
| 10 | trans | δ,δ,δ,δ,δ,δ | 24.1 | -0.20407 | -2901.34381 | 9.5 |
| 11 | cis | δ,δ,δ,λ,δ,δ | 39.7 | -0.20301 | -2901.33680 | 27.9 |
| 12 | cis | δ,δ,δ,λ,λ,δ | 32.8 | -0.20782 | -2901.34425 | 8.3 |
| 13 | trans | δ,λ,λ,δ,δ,λ | 27.7 | -0.20466 | -2901.34300 | 11.6 |

**Table S2.** Calculated $\Delta G_{gas}$, $\Delta G_{solv}$, $G_{soln}$ and $\Delta G_{soln}$ energies for all investigated conformers of the **[Hg($N_2S_4$-Thio)]$^{2+}$** complex. The lowest energy conformation is highlighted in bold.

| Conformer | Sidearm Orientation | Backbone | Relative $G_{gas}$ (kJ/mol) | $\Delta G_{solv}$ (Hartree) | $G_{soln}$ (Hartree) | Relative $G_{soln}$ (kJ/mol) |
|---|---|---|---|---|---|---|
| 1 | cis | δ,λ,δ,λ,δ,λ | 45.2 | -0.21420 | -3360.75521 | 45.7 |
| 2 | trans | λ,δ,λ,λ,λ,λ | 61.1 | -0.21687 | -3360.75183 | 54.6 |
| 3 | cis | λ,δ,δ,λ,λ,δ | 43.4 | -0.22067 | -3360.76237 | 26.9 |
| 4 | trans | λ,δ,δ,λ,λ,λ | 19.7 | -0.21606 | -3360.76678 | 15.4 |
| 5 | cis | λ,δ,λ,δ,λ,δ | 19.0 | -0.21819 | -3360.76918 | 9.1 |
| 6 | trans | λ,δ,λ,λ,δ,δ | 24.0 | -0.20793 | -3360.75701 | 41.0 |
| **7** | **cis** | **δ,λ,δ,λ,δ,λ** | **9.8** | **-0.21816** | **-3360.77263** | **0.0** |
| 8 | cis | λ,λ,λ,δ,λ,δ | 37.7 | -0.22318 | -3360.76702 | 14.7 |
| 9 | trans | λ,λ,λ,λ,λ,λ | 61.1 | -0.21687 | -3360.75183 | 54.6 |
| 10 | cis | λ,λ,δ,λ,λ,δ | 19.0 | -0.21488 | -3360.76585 | 17.8 |
| 11 | cis | λ,δ,δ,δ,λ,δ | 0.0 | -0.20560 | -3360.76381 | 23.2 |

**Table S3.** Calculated $\Delta G_{gas}$, $\Delta G_{solv}$, $G_{soln}$ and $\Delta G_{soln}$ energies for all investigated conformers of the **[Hg($N_2S_4$-Pa)]** complex. The lowest energy conformation is highlighted in bold.

| Conformer | Sidearm Orientation | Backbone | Relative $\Delta G_{gas}$ (kJ/mol) | $\Delta G_{solv}$ (Hartree) | $G_{soln}$ (Hartree) | Relative $\Delta G_{soln}$ (kJ/mol) |
|---|---|---|---|---|---|---|
| 1 | Cis | δ,δ,λ,δ,λ,λ | 67.9 | -0.03788 | -3277.69609 | 58.2 |
| 2 | Trans | δ,δ,δ,λ,δ,λ | 47.1 | -0.04202 | -3277.70814 | 26.6 |
| 3 | Cis | λ,δ,δ,δ,λ,δ | 33.6 | -0.04562 | -3277.71688 | 3.6 |
| 4 | Trans | δ,λ,δ,λ,δ,λ | 76.6 | -0.03391 | -3277.68878 | 77.4 |
| 5 | Cis | δ,δ,δ,λ,δ,λ | 32.8 | -0.04081 | -3277.71239 | 15.4 |
| 6 | Trans | λ,λ,δ,λ,δ,λ | 123.8 | -0.04292 | -3277.67984 | 100.9 |
| **7** | **Cis** | **δ,δ,λ,δ,δ,δ** | **0.0** | **-0.03421** | **-3277.71827** | **0.0** |
| 8 | Trans | δ,λ,δ,δ,λ,λ | 54.4 | -0.02791 | -3277.69124 | 71.0 |
| 9 | Cis | λ,λ,δ,δ,δ,λ | 0.6 | -0.03383 | -3277.71767 | 1.6 |
| 10 | Trans | δ,δ,δ,λ,λ,λ | 35.7 | -0.03808 | -3277.70854 | 25.5 |
| 11 | Cis | δ,δ,λ,δ,δ,λ | 37.9 | -0.04314 | -3277.71278 | 14.4 |

**Table S4.** Selected bond angles and distances for conformers 5 ($\Delta G_{gas}$= 0 kJ/mol) and 9 ($\Delta G_{soln}$= 0 kJ/mol) of the **[Hg($N_2S_4$-Py)]$^{2+}$** complex.

| Bond Length (Å) | | | Bond Angle (°) | | |
|---|---|---|---|---|---|
| | **Conformer 5** | **Conformer 9** | | **Conformer 5** | **Conformer 9** |
| **S1-Hg** | 2.909 | 2.724 | **S1-Hg-S2** | 75.6 | 78.3 |
| **S2-Hg** | 2.823 | 2.925 | **S2-Hg-N4** | 62.7 | 70.1 |
| **S3-Hg** | 2.841 | 2.773 | **N4-Hg-S3** | 66.1 | 75.9 |
| **S4-Hg** | 2.852 | 4.321 | **S3-Hg-S4** | 77.6 | 56.8 |
| **N1-Hg** | 2.985 | 2.934 | **S4-Hg-N1** | 67.7 | 53.6 |
| **N2-Hg** | 2.501 | 2.436 | **N1-Hg-S1** | 63.7 | 71.4 |
| **N3-Hg** | 2.525 | 2.539 | | | |
| **N4-Hg** | 3.000 | 2.693 | | | |

**Table S5.** Selected bond angles and distances for conformers 7 ($\Delta G_{gas}$= 0 kJ/mol) and 11 ($\Delta G_{soln}$= 0 kJ/mol) of the **[Hg($N_2S_4$-Thio)]$^{2+}$** complex.

| Bond Length (Å) | | | Bond Angle (°) | | |
|---|---|---|---|---|---|
| | **Conformer 11** | **Conformer 7** | | **Conformer 11** | **Conformer 7** |
| **S1-Hg** | 2.939 | 2.941 | **S1-Hg-S2** | 71.5 | 76.3 |
| **S2-Hg** | 2.857 | 2.767 | **S2-Hg-N2** | 67.8 | 66.4 |
| **S3-Hg** | 2.861 | 2.596 | **N2-Hg-S3** | 69.1 | 62.2 |
| **S4-Hg** | 2.696 | 3.898 | **S3-Hg-S4** | 78.5 | 56.3 |
| **S5-Hg** | 2.961 | 2.658 | **S4-Hg-N1** | 57.4 | 50.6 |
| **S6-Hg** | 2.698 | 2.787 | **N1-Hg-S1** | 54.9 | 56.4 |
| **N1-Hg** | 3.755 | 3.858 | | | |
| **N2-Hg** | 3.031 | 3.166 | | | |

**Table S6.** Selected bond angles and distances for conformer 11, 7 and 3 ($\Delta G_{gas}$= 0 kJ/mol) and 9 ($\Delta G_{soln}$= 0 kJ/mol) of the **[$^{nat}$Hg][Hg($N_2S_4$-Pa)]** complex.

| Bond Length (Å) | | | | Bond Length (Å) | | | |
|---|---|---|---|---|---|---|---|
| | **Conf. 11** | **Conf. 7** | **Conf. 3** | | **Conf. 11** | **Conf. 7** | **Conf 3.** |
| **S1-Hg** | 2.659 | 3.905 | 2.737 | **O1-Hg** | 2.471 | 2.445 | 2.378 |
| **S2-Hg** | 3.693 | 2.756 | 4.022 | **O2-Hg** | 2.380 | 2.431 | 2.413 |
| **S3-Hg** | 3.408 | 3.994 | 4.753 | **N2-Hg** | 2.524 | 2.482 | 2.444 |
| **S4-Hg** | 4.218 | 2.731 | 2.737 | **N3-Hg** | 2.450 | 2.542 | 2.417 |
| **N1-Hg** | 3.052 | 3.111 | 2.938 | **N4-Hg** | 3.070 | 3.238 | 3.684 |

## Radiolabeling and Stability

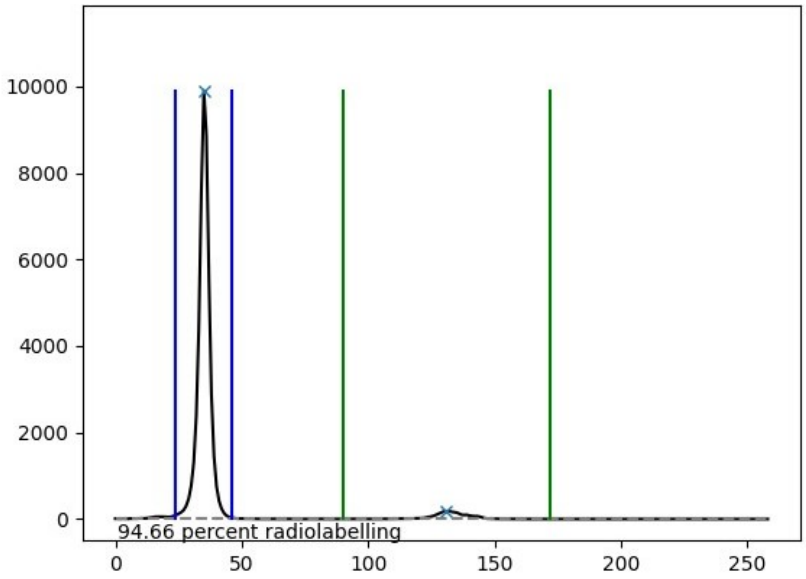


**Figure S27.** iTLC of $N_2S_4$-Thio at $10^{-4}$ M, showing 94.7% RCY at 80 ºC.

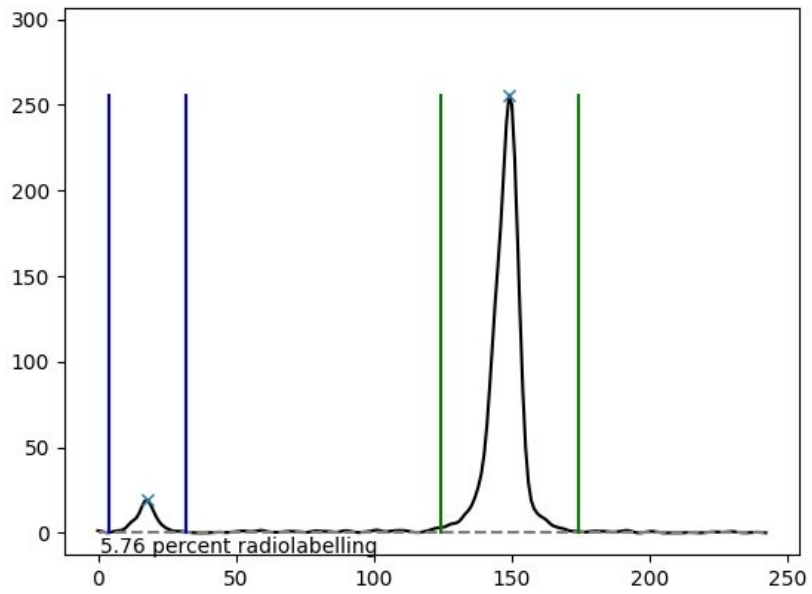


**Figure S28.** iTLC of $N_2S_4$-Thio at $10^{-6}$ M, showing 5.8 % RCY at 80 ºC.

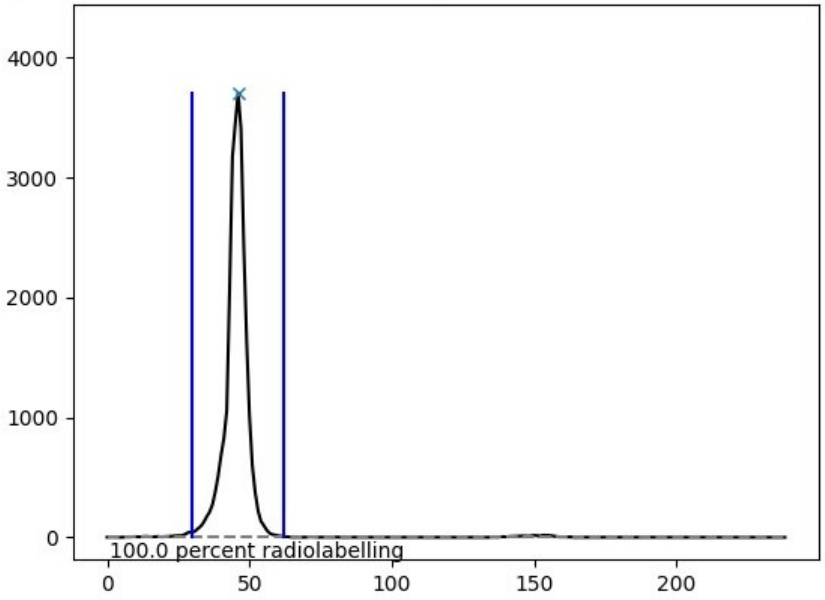


**Figure S29.** iTLC of $N_2S_4$-Py at $10^{-4}$ M, showing 100 % RCY at 80 ºC.

**Table S7.** Average RCYs (%) of [$^{197m/g}$Hg]Hg-Complexes at 80 °C after 60 min, in 1 M $NH_4OAc$ buffer (pH 7).

| %RCY | Concentration (M) | | | |
|---|---|---|---|---|
| | $10^{-4}$ | $10^{-5}$ | $10^{-6}$ | $10^{-7}$ |
| **[$^{197m/g}$Hg][Hg($N_2S_4$-Py)]$^{2+}$** | 100.0 ± 0.0% | 86.2 ± 1.9 % | 17.3 ± 6.6 % | 6.3 ± 2.4 % |
| **[$^{197m/g}$Hg][Hg($N_2S_4$-Thio)]$^{2+}$** | 96.8 ± 0.5% | 65.0 ± 4.5 % | 11.9 ± 9.0 % | 6.4 ± 1.0 % |
| **[$^{197m/g}$Hg][Hg($N_2S_4$-Pa)]$^{2+}$** | 26.0 ± 1.3% | - | - | - |
| **[$^{197m/g}$Hg][Hg($NS_4$-BA)]$^{2+}$*** | 100.0 ± 0.0% | 97.0 ± 0.3 % | 31.3 ± 2.0 % | - |

*[$^{197m/g}$Hg][Hg($NS_4$-BA)]$^{2+}$ radiolabeling data is reproduced from Randhawa *et al.* after 1 h.[1]

**Table S8.** Average RCYs (%) of [$^{197m/g}$Hg]Hg-Complexes at 25 °C after 60 min, in 1 M $NH_4OAc$ buffer (pH 7).

| %RCY | Concentration (M) | | | |
|---|---|---|---|---|
| | $10^{-4}$ | $10^{-5}$ | $10^{-6}$ | $10^{-7}$ |
| **[$^{197m/g}$Hg][Hg($N_2S_4$-Py)]$^{2+}$** | 37.0 ± 3.3 % | - | - | - |
| **[$^{197m/g}$Hg][Hg($N_2S_4$-Thio)]$^{2+}$** | 95.5 ± 1.8 % | 12.3 ± 2.6 % | 5.3 ± 4.0 % | - |
| **[$^{197m/g}$Hg][Hg($N_2S_4$-Pa)]$^{2+}$** | 33.1 ± 0.2 % | - | - | - |

**Table S9.** Kinetic inertness of [$^{197m/g}$Hg]Hg-Complexes at 37 °C against human serum. ($n$=3)

| $^{197m/g}$Hg-complex % intact | Time point (h) | | | | |
|---|---|---|---|---|---|
| | 1 | 3 | 16 | 24 | 72 |
| **[$^{197m/g}$Hg][Hg($N_2S_4$-Py)]$^{2+}$** | 71. ± 2.2 % | 57.2 ± 8.2 % | 58.9 ± 8.7 % | - | 65.1 ± 1.5 % |
| **[$^{197m/g}$Hg][Hg($N_2S_4$-Thio)]$^{2+}$** | 75.5 ± 0.8 % | 67.8 ± 5.0 % | 70.8 ± 0.1 % | - | 60.3 ± 2.1 % |
| **[$^{197m/g}$Hg][Hg($NS_4$-BA)]$^{2+}$*** | 84.7 ± 3.4 % | 74.1 ± 7.0 % | - | - | - |

*[$^{197m/g}$Hg][Hg($NS_4$-BA)]$^{2+}$ radiolabeling data is reproduced from Randhawa *et al.* after 1 h.[1]

**Table S10.** Kinetic inertness of [$^{197m/g}$Hg]Hg-Complexes at 37 °C against GSH. (*n*=3)

| $^{197m/g}$Hg-complex % intact | Time point (h) | | | | |
|---|---|---|---|---|---|
| | 1 | 3 | 10 | 24 | 72 |
| **[$^{197m/g}$Hg][Hg($N_2S_4$-Py)]$^{2+}$** | 85.8 ± 0.4 % | 72.6 ± 0.4 % | - | 32.0 ± 5.1% | - |
| **[$^{197m/g}$Hg][Hg($N_2S_4$-Thio)]$^{2+}$** | 77.8 ± 0.4 % | 75.1 ± 3.0 % | - | 43.7 ± 3.2% | - |
| **[$^{197m/g}$Hg][Hg($NS_4$-BA)]$^{2+}$*** | 100.0 ± 0.0 % | - | 97.3 ± 0.3 % | - | 92.3 ± 0.5 % |

*[$^{197m/g}$Hg][Hg($NS_4$-BA)]$^{2+}$ radiolabeling data is reproduced from Randhawa *et al.* after 1 h.[1]

**Table S11.** Kinetic inertness of [$^{197m/g}$Hg]Hg-Complexes at 25 °C against stable biologically relevant metals ($ZnCl_2$, $FeCl_3$, $CuCl_2$, $MgCl_2$ and $CoCl_2$). (*n*=3)

| $^{197m/g}$Hg-complex % intact | Time point (h) | | |
|---|---|---|---|
| | 24 | 48 | 85 |
| **[$^{197m/g}$Hg][Hg($N_2S_4$-Py)]$^{2+}$** | 90.8 ± 8.7 % | 83.9 ± 5.0 % | 73.0 ± 7.0 % |
| **[$^{197m/g}$Hg][Hg($N_2S_4$-Thio)]$^{2+}$** | 86.2 ± 1.7 % | 86.0 ± 2.6 % | 86.9 ± 3.2 % |

## References


(1) Gonçalves, P. F. B.; Stassen, H. Calculation of the Free Energy of Solvation from Molecular Dynamics Simulations. *Pure Appl. Chem.* **2004**, *76* (1), 231–240. https://doi.org/10.1351/pac200476010231.

(2) Randhawa, P.; Gower-Fry, K. L.; Stienstra, C. M. K.; Tosato, M.; Chen, S.; Gao, Y.; McDonagh, A. W.; Di Marco, V.; Radchenko, V.; Schreckenbach, G.; Ramogida, C. F. Selective Chelation of the Exotic Meitner-Auger Emitter Mercury-197m/g with Sulfur-Rich Macrocyclic Ligands: Towards the Future of Theranostic Radiopharmaceuticals. *Chem. – Eur. J.* **2023**, *29* (21), e202203815. https://doi.org/10.1002/chem.202203815.